STATE-SPACE FILTERS

BASED ON

LC LADDER SIMULATION

by

David A. Johns

A thesis submitted to the Department of Electrical Engineering
in conformity with the requirements for the degree
of Master of Applied Science

University of Toronto

Toronto, Ontario

September, 1983

ACKNOWLEDGEMENTS

I would like to express my sincere thanks to my supervisor, Professor Adel Sedra. Without his guidance, the material contained in this thesis might not have been possible. Also his excellent advice on the presentation of this thesis is much appreciated. I am also indebted to Martin Snelgrove who produced the basis for this thesis and contributed with helpful advice.

Also I would like to acknowledge the finanial support provided to me by NSERC through a Postgraduate Scholarship.

ABSTRACT

This thesis is concerned with the application of the recently introduced Intermediate-Function (IF) synthesis to the design of active filters that simulate LC ladder prototypes. IF synthesis results in filter realizations composed of integrators connected together with resistive feedback and feedforward paths. Such filters are most conveniently described in terms of the state-variable formulation and are referred to as State-Space filters.

The material contained herein consists of two parts. Firstly, experimental evidence is given which verifies the sensitivity and dynamic range formulae of IF synthesis. Secondly, a simple systematic design approach is presented for active RC state-space filters. The resulting canonic filters simulate the operation of LC ladder prototypes, both canonic and non-canonic. In the latter case, it is shown that care must be exercised in selecting the ladder states that the active filters simulate, otherwise performance is seriously compromised. The sensitivity and dynamic range performance of the resulting filter is shown to be superior to that obtained with other ladder simulation techniques.

TABLE OF CONTENTS

1. INTRODUCTION

This thesis attempts to make two contributions to existing filter design theory. One contribution is to provide experimental verification of the sensitivity and noise analysis presented by Martin Snelgrove [1] for state-space active filters. In this thesis, this analysis will be verified through the use of active RC state-space filters which simulate LC ladders.

The second contribution is to provide a simple new design method for obtaining an active RC filter which simulates the operation of a passive LC ladder prototype. The method is called "State-space LC ladder simulation". The LC ladder prototype is typically a doubly-terminated LC network which has good sensitivity properties in the passband. The good sensitivity properties result from the fact that a doubly-terminated ladder is designed for maximum power transfer at reflection zeros and therefore if any of the ladder's components deviate from their nominal value, the passband gain will decrease. This implies that the first-order sensitivity of the transfer function to any element in the ladder is zero at all reflection zeros [2].

It is presently common practice to design most high-order filters based on LC ladder prototypes. For canonic ladders, the method used most often to simulate the ladder is the Leap-Frog approach [3]. This method works quite well in maintaining the low sensitivity properties of the canonic ladder with no apparent problems. State-space LC ladder simulations produce the same active filter structure as the Leap-Frog approach. Problems arise, however, when one

attempts to simulate a non-canonic ladder, with the result that almost all of the design methods now in use have some difficulties associated with them. Four of the current design methods for dealing with non-canonic ladders are discussed briefly below.

The Signal Flow Graph (SFG) [4,5] method makes use of reciprocators which are in effect differentiators. The reciprocators are often difficult to compensate and add high frequency noise to the active filter. The SFG design method is, nevertheless, a very systematic design approach and can be applied to any LC ladder prototype.

Another method is to actively simulate all inductors in the ladder through the use of Generalized Immittance Converters (GIC) [5,6]. This method has the problem that it is very dependent on the passive LC ladder used as a prototype. If the ladder is not designed properly, then the GIC simulation will most likely have poor dynamic range performance.

A third method is a variation of the Leap-Frog approach, known as the "capacitor-splitting" method [7], which can simulate the operation of certain classes of LC ladders. This method appears to work well on low-pass filters though some network transformations must be applied to the LC ladder prototype. Furthermore, for this method to work, the ladder prototype must be in a certain configuration.

A final approach is multiple-feedback active filters [8]. This method does not simulate an LC ladder prototype but rather tries to obtain a realization of the transfer function which could have been derived from some LC ladder. In many

cases, the corresponding LC ladder is unrealizable with passive immittances so it is not clear that this method maintains the low sensitivity properties of doubly-terminated LC ladders.

State-space LC ladder simulation allows one to easily design an active filter from a given ladder prototype. The prototype may be any doubly-terminated LC ladder. The resulting filter will have the same low sensitivity properties as the present best LC ladder simulation. Perhaps an even more important property of state-space filters is that first-order sensitivity formulae can be easily derived for any element in the active filter. As well, the output noise voltage can be accurately predicted if we know the input noise voltage of the op-amps to be used in implementation. A state-space LC ladder simulation filter has the advantage over other state-space filters in that its system matrix is quite sparse and is easy to design. (If the system matrix is sparse, there are fewer components needed in the circuit realization.)

State-space LC ladder simulation is a canonic simulation of the LC ladder prototype. N independent states are required to create a transfer function of order N. These N states are formed at the output of N integrators connected with feed-forward and feedback networks. Each of the states is a simulation of a capacitor voltage or inductor current in the LC ladder. If the LC ladder is non-canonic then the number of reactive elements is greater than the order of the filter, N. In this case, N states are required in the simulation so some capacitor voltages or inductor currents are not simulated. We say that these states have not been chosen to be simulated.

The choice of the states from a non-canonic ladder can lead to good and bad filters. In some cases, the transfer function is unrealizable because one chooses two states which are dependent. Since the choice of states is quite important, a full chapter is devoted to helping one make this choice.

1.1 Thesis Outline

The theory required for this thesis is contained in chapter 2. This theory is not restricted to the state-space LC ladder simulation technique but is applicable for state-space filters in general. Sensitivity equations are given for most circuit components in a state-space filter, and as well, an equation is presented which predicts the deviation in the transfer function resulting from the op-amp's finite gain.

Chapter 3 shows experimental verification of the formulae presented in chapter 2 obtained from [1]. It is very impressive that the sensitivity and output noise results can be so accurately predicted.

The succeeding two chapters deal exclusively with LC ladder simulations in state-space systems. Chapter 4 attempts to provide some insight as to which states should be simulated for a non-canonic ladder. Only N states are required in the simulation yet a non-canonic ladder has greater than N possible states. A rule-of-thumb is presented which appears to give good results for all filters simulated so far.

Chapter 5 gives the design details of how one obtains the state-space system from an LC ladder once one has decided on which states to simulate. Two approaches are presented, one which is well-suited to computers and one which can be performed easily by hand calculations.

The final chapter presents conclusions and outlines possible areas for further study.

2. THEORY

This chapter presents formulae which are used in the analysis of state-space systems. Also presented is a general state-space active RC circuit and formulae which show the sensitivity of the filter transfer function to variations in the circuit elements and op-amp gain-bandwidth.

2.1 The State-Space Description

A conventional N'th order state-space system is described by the equations:

$$\dot{\mathbf{x}}(t) = \mathbf{A}\mathbf{x}(t) + \mathbf{b}u(t) \tag{2-1}$$

$$y(t) = \mathbf{c}^{\mathbf{T}}\mathbf{x}(t) + du(t) \tag{2-2}$$

where "u" is the input signal; "$\mathbf{x}$" is a vector of N states, which in our case, are the integrator outputs; and "y" is the output signal. $\mathbf{A}$, $\mathbf{b}$, $\mathbf{c}$, and d are the coefficients relating these variables. "$\mathbf{A}$" is a N x N real matrix which determines the feedforward and feedback of the N integrators. "$\mathbf{b}$" and "$\mathbf{c}$" are N x 1 real vectors which determine the input and output signals to the filter. "d" is a scalar which allows a direct feedthrough from the input to the output.

Writing (2-1) in Laplace form and solving for $\mathbf{x}$ in terms of u gives the following equation[1]

$$\mathbf{x} = (s\mathrm{I}-\mathrm{A})^{-1}\mathbf{b}u \tag{2-3}$$

Substituting (2-3) into (2-2) and dividing both sides by u gives the transfer function of the filter as:

$$T(s) = \frac{y(s)}{u(s)} = \mathbf{c}^T(s\mathrm{I}-\mathrm{A})^{-1}\mathbf{b}+d \tag{2-4}$$

2.2 Intermediate-Transfer Functions

For sensitivity equations we need to define two other transfer functions, $f_i(s)$ and $g_i(s)$.

Defining $f_i(s)$ to be the transfer function from system input to the output of the i'th integrator then one can see from (2-3) that:

---

1. The same symbols will be used for frequency and time domains, but time domain quantities will be explicitly indicated through the use of (t).

$$\mathbf{f}(s) = \frac{\mathbf{x}(s)}{u(s)} = (s\,\mathbf{I}-\mathbf{A})^{-1}\mathbf{b} \tag{2-5}$$

The above set of functions are called the *intermediate-transfer functions*.

A dual function, $g_i(s)$, is defined as the transfer function from the input of the i'th integrator, $\dot{x}_i(t)$, to the system output, $y(t)$. We find $g_i(s)$ by reducing the input to zero and injecting a signal, ξ_i, at sx_i. The state equations become:

$$s\mathbf{x} = \mathbf{A}\mathbf{x}+\xi \tag{2-6}$$

$$y = \mathbf{c}^{\mathbf{T}}\mathbf{x} \tag{2-7}$$

So the set of functions, $g_i(s)$, is found to be:

$$\mathbf{g}^{\mathbf{T}}(\mathbf{s}) = \frac{y(s)}{\xi(s)} = \mathbf{c}^{\mathbf{T}}(s\,\mathbf{I}-\mathbf{A})^{-1} \tag{2-8}$$

All the functions $T(s)$, $f_i(s)$, and $g_i(s)$ share the same denominator -- the natural mode polynomial, e(s). One can also find a matrix representation for both $\{f_i(s)\}$ and $\{g_i(s)\}$ and then find a simple formula relating the two matrices.

First looking at $f_1(s)$

$$f_1(s) = \frac{n_1(s)}{e(s)} \tag{2-9}$$

writing $e(s)$ as a product of its roots gives

$$f_1(s) = \frac{n_1(s)}{(s-e_1)(s-e_2)\ldots(s-e_N)} \tag{2-10}$$

where e_i is the i'th root of the natural mode polynomial, $e(s)$.

Now using partial fraction expansion, one can write $f_1(s)$ as

$$f_1(s) = \frac{F_{11}}{(s-e_1)} + \frac{F_{12}}{(s-e_2)} + \cdots + \frac{F_{1N}}{(s-e_N)} \tag{2-11}$$

where F_{ij} are in general numbers (no "s" terms).

Similarly

$$f_2(s) = \frac{F_{21}}{(s-e_1)} + \frac{F_{22}}{(s-e_2)} + \cdots + \frac{F_{2N}}{(s-e_N)} \tag{2-12}$$

$$f_N(s) = \frac{F_{N1}}{(s-e_1)} + \frac{F_{N2}}{(s-e_2)} + \cdots + \frac{F_{NN}}{(s-e_N)} \tag{2-13}$$

so finally, one can write

$$\mathbf{f}(s) = \mathbf{F}\mathbf{e}(s) \tag{2-14}$$

where

$$\mathbf{f}(s) = \begin{bmatrix} f_1 \\ f_2 \\ \cdot \\ \cdot \\ f_N \end{bmatrix} \quad \mathbf{F} = \begin{bmatrix} F_{11}\ F_{12}\ \cdot\ \cdot\ F_{1N} \\ F_{21}\ F_{22} \quad\quad F_{2N} \\ \cdot \quad\quad\quad\quad \cdot \\ \cdot \quad\quad\quad\quad \cdot \\ F_{N1}\ F_{N2}\ \cdot\ \cdot\ F_{NN} \end{bmatrix} \quad \mathbf{e}(s) = \begin{bmatrix} \frac{1}{s-e_1} \\ \frac{1}{s-e_2} \\ \cdot \\ \cdot \\ \frac{1}{s-e_N} \end{bmatrix} \tag{2-15}$$

Using the same method and similar notation, one can find an N x N matrix, **G**, such that

$$\mathbf{g}(s) = \mathbf{G}\mathbf{e}(s) \tag{2-16}$$

A formula is derived in [1] which states that

$$\mathbf{G}^T = \mathbf{H}\mathbf{F}^{-1} \tag{2-17}$$

where H is a diagonal N x N matrix such that

$$T(s) = \mathrm{He}(s). \quad T(s) \textit{ is the transfer function} \tag{2-18}$$

This is an important formula since it aids in the computation of either **F** or **G** as well as giving insight as to why some choices of intermediate-transfer functions are bad.

2.3 Sensitivities

The formula to derive sensitivities using **f** and **g** is (cf. fig. 2.1):

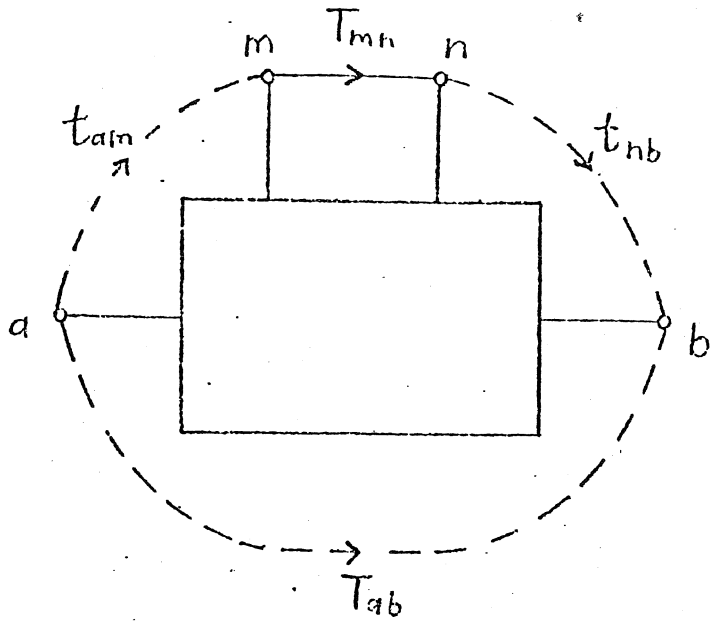

Figure 2.1 Investigating one arm of a signal flow graph which illustrates the transfer functions of formula (2-19).

$$\frac{dT_{ab}}{dT_{mn}} = t_{am} \cdot t_{nb} \qquad (2\text{-}19)$$

where t_{am}, eg., is the transfer function from point "a" to point "m". The proof of this formula is given in [1].

If we use the classical sensitivity measure

$$S_{T_{mn}}^{T_{ab}} = \frac{dT_{ab}}{dT_{mn}} \cdot \frac{T_{mn}}{T_{ab}} \qquad (2\text{-}20)$$

then

$$S_{T_{mn}}^{T_{ab}} = t_{am} \cdot t_{nb} \frac{T_{mn}}{T_{ab}} \tag{2-21}$$

Fig. 2.2 shows how **A**, **b**, **c**, and d relate to formula (2-19) giving the following formulae:

$$S_{A_{ij}}^{T(s)} = g_i f_j \cdot \frac{A_{ij}}{T(s)} \tag{2-22}$$

$$S_{b_i}^{T(s)} = g_i \cdot \frac{b_i}{T(s)} \tag{2-23}$$

$$S_{c_i}^{T(s)} = f_i \cdot \frac{c_i}{T(s)} \tag{2-24}$$

$$S_{d}^{T(s)} = \frac{d}{T(s)} \tag{2-25}$$

The next section will show formulae relating matrix elements and circuit component values. These can be used to find the sensitivity formulae of matrix elements to variations in circuit components. The resulting formulae are then combined with the above sensitivity formulae to give formulae which show the sensitivity of the transfer function to variations in circuit element values.

The final sensitivity formula derived will be for integrators. Toward that end, we model each integrator as an ideal integrator in cascade with a block having a transfer function γ_i which contains all the integrator non-idealities as well as the integrator gain. In the state-space system the integrator transfer function is simply $\frac{1}{s}$ so γ_i is nominally one. However in the active circuit the integrator

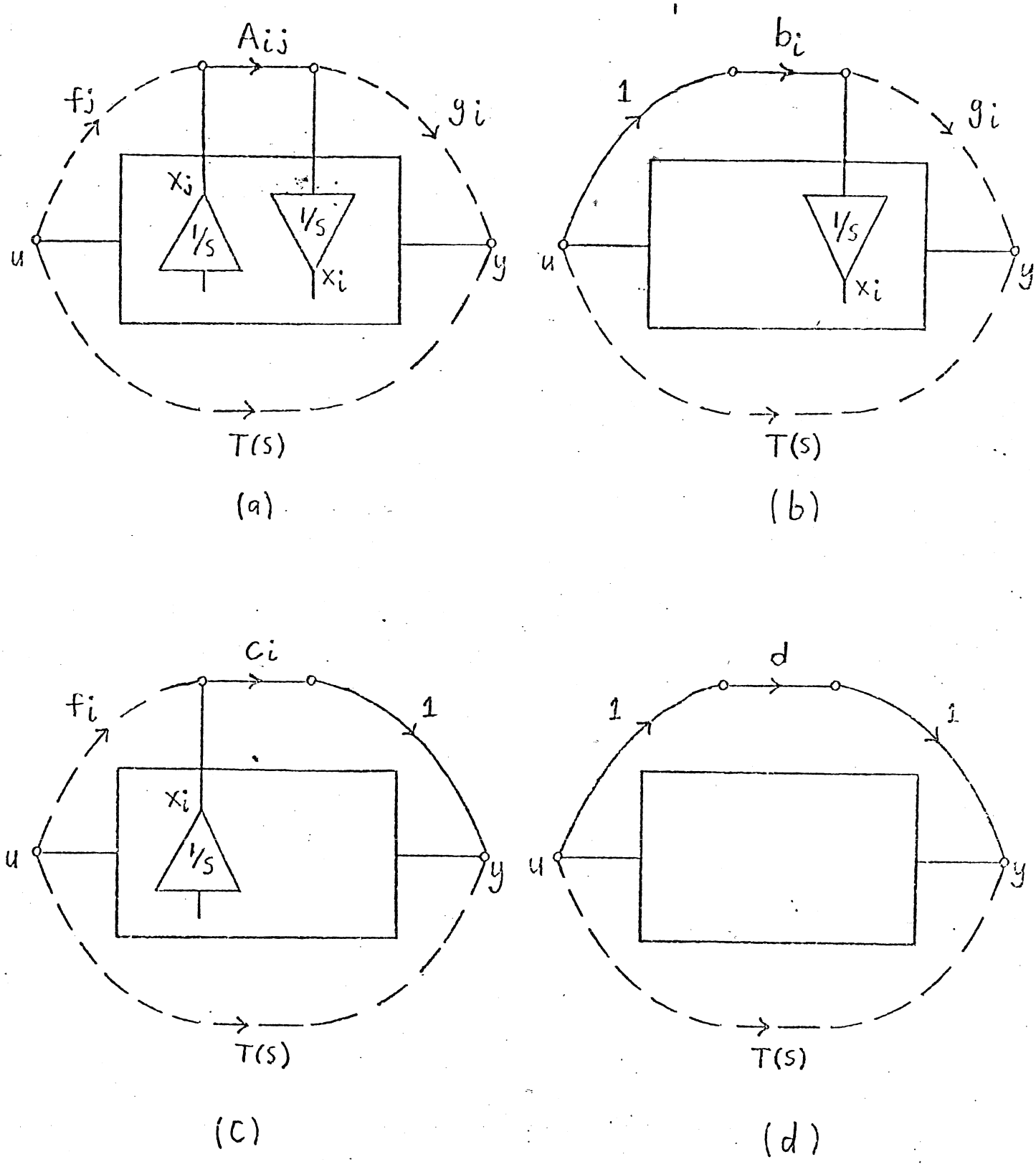

Figure 2.2 SFG representations used to detemine matrix element sensitivity formulae

gain and hence γ_i is scaled to denormalize the filter. Then each integrator of the system has the transfer function:

$$\frac{V_o}{V_i} = \frac{-1}{s}\gamma_i \tag{2-26}$$

Fig 2.3 shows how γ_i relates to formula (2-19). Note that t_{nb} is sg_i because g_i is the transfer function from the input not the output of integrator "i".

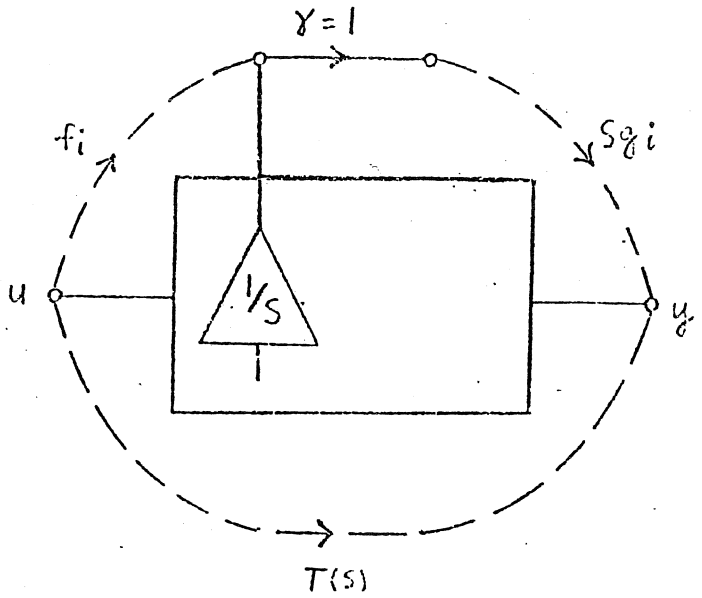

Figure 2.3 SFG representation used to determine integrator sensitivity shown in formula (2-27)

The sensitivity of the transfer function to γ_i is:

$$S_{\gamma_i}^{T(s)} = f_i g_i \frac{s}{T(s)} \tag{2-27}$$

All of the formulae above relate the sensitivity of a complex function, the transfer function, to possible complex functions, eg. γ_i. For analysis of filters, it is usually the case that one would like to predict the variations in the magnitude of the transfer function as a result of variations in the magnitude or phase of parameters. The real and imaginary parts of the sensitivity of complex functions are taken to obtain formulae involving the magnitude and phase of these functions. These formulae are derived with the aid of Cauchy-Riemann equations.

A modified theorem involving Cauchy-Riemann equations states that: If a complex function $q(s)$

$$q(s) = w(s)+jv(s) \tag{2-28}$$

($w(s)$ and $v(s)$ are real functions) is analytic in D where D is a surface in

$$z(s) = x(s)+jy(s) \tag{2-29}$$

($z(s)$ is an analytic function , $x(s)$ and $y(s)$ are real analytic functions) then $w(s)$ and $v(s)$ have continuous first partial derivatives in D and satisfy

$$\frac{\partial q(s)}{\partial z(s)} = \frac{\partial w(s)}{\partial x(s)} + j\frac{\partial v(s)}{\partial x(s)} = \frac{\partial v(s)}{\partial y(s)} - j\frac{\partial w(s)}{\partial x(s)} \tag{2-30}$$

To relate the above to the sensitivity equations first write $T(s)$ as

$$T(s) = |T(s)|\, e^{j\varphi[T(s)]} \tag{2-31}$$

where $|T(s)|$ and $\varphi[T(s)]$ are the magnitude and phase of $T(s)$ respectively, then

$$\ln[T(s)] = \ln|T(s)| + j\varphi[T(s)] \tag{2-32}$$

Similarly, for any complex parameter, call it $\mu(s)$.

$$\ln[u(s)] = \ln|\mu(s)| + j\varphi[\mu(s)] \tag{2-33}$$

Relating $\ln|T(s)|$ to $w(s)$, $\varphi[T(s)]$ to $v(s)$, $\ln|\mu(s)|$ to $x(s)$, and $\varphi[\mu(s)]$ to $y(s)$ we find the following equations

$$S_{\mu(s)}^{T(s)} = \frac{\partial \ln[T(s)]}{\partial \ln[\mu(s)]} = \frac{\partial \ln|T(s)|}{\partial \ln|\mu(s)|} + j\frac{\partial \varphi[T(s)]}{\partial \ln|\mu(s)|} \tag{2-34}$$

$$= \frac{\partial \varphi[T(s)]}{\partial \varphi[\mu(s)]} - j\frac{\partial \ln|T(s)|}{\partial \varphi[\mu(s)]} \tag{2-35}$$

Looking at real and imaginary parts separately, this gives

$$\mathrm{Re}\left[S_{\mu(s)}^{T(s)}\right] = \frac{\partial \ln|T(s)|}{\partial \ln|\mu(s)|} = S_{|\mu(s)|}^{|T(s)|} \tag{2-36}$$

$$= \frac{\partial \varphi[T(s)]}{\partial \varphi[\mu(s)]} \tag{2-37}$$

$$\mathrm{Im}\left[S_{\mu(s)}^{T(s)}\right] = -\frac{\partial \ln|T(s)|}{\partial \varphi[\mu(s)]} \tag{2-38}$$

$$= \frac{\partial \varphi[T(s)]}{\partial \ln|\mu(s)|} \tag{2-39}$$

2.4 Scaling of a State-Space System

While maintaining the same transfer function, it is often useful to scale the set of intermediate-transfer functions, $\{f_i\}$, in a state-space system by the values α_1, α_2, etc., where f_i is scaled by α_i. It is well known that the transfer function is not changed under the similarity transformation which is defined as a transformation from a system with matrices

$$(\mathbf{A},\mathbf{b},\mathbf{c},d)$$

to one with matrices

$$(\mathbf{TAT}^{-1},\mathbf{Tb},\mathbf{cT}^{-1},d) \triangleq (\hat{\mathbf{A}},\hat{\mathbf{b}},\hat{\mathbf{c}},\hat{d}) \tag{2-40}$$

where **T** is a non-singular N x N matrix.

If **T** is simply a diagonal matrix such as

$$\mathbf{T} = \begin{bmatrix} \alpha_1 & 0 & \cdot & \cdot & 0 \\ 0 & \alpha_2 & 0 & \cdot & \cdot \\ \cdot & 0 & \alpha_3 & 0 & \cdot \\ \cdot & \cdot & 0 & \cdot & 0 \\ 0 & \cdot & \cdot & 0 & \alpha_N \end{bmatrix} \tag{2-41}$$

then a similarity transformation with this **T** is a method of scaling the intermediate-transfer functions in the state-space system.

The scaled-system elements become

$$\hat{A}_{ij} = \frac{\alpha_i}{\alpha_j} A_{ij} \qquad \hat{b}_i = \alpha_i b_i \tag{2-42}$$

$$\hat{c}_j = \frac{c_j}{\alpha_j} \qquad \hat{d} = d \tag{2-43}$$

While the set $\{f_i\}$ and the set $\{g_i\}$ become

$$\hat{f}_i = \alpha_i f_i \qquad \hat{g}_i = \frac{g_i}{\alpha_i} \tag{2-44}$$

Note that scaling a state-space system does not affect any of its sensitivity properties.[2] As an example, let us use the relationship in equation (2-22) together with (2-42) to compare the sensitivity of the scaled system relative to A_{ij},

---

2. It will be shown later, however, that scaling does in fact affect the sensitivity of the circuit transfer function relative to the finite gain of the op-amps due to the fact that the closed-loop gain of each integrator (ie. time-constant) is changed.

$$S_{A_{ij}}^{T(s)} = \frac{g_i}{\alpha_i}\alpha_j f_j \cdot \frac{\alpha_i A_{ij}}{\alpha_j T(s)} \tag{2-45}$$

$$= g_i f_j \cdot \frac{A_{ij}}{T(s)} = S_{A_{ij}}^{T(s)} \tag{2-46}$$

2.5 Circuit Implementation and Sensitivity

Figure 2.4 shows a direct circuit realization of an N'th order state-space filter. The output of integrator i is the state $-X_i$. Within arbitrary values for C_i and R_{yy} there is a one to one correspondence between the filter component values and the system element values, $\mathbf{A}$, $\mathbf{b}$, $\mathbf{c}^T$, and d. Typically, one will design a filter with normalized specifications where the upper passband edge is at $1\,rad/sec$. To denormalize the state-space system, one chooses R_i and C_i so that

$$\omega_n R_i C_i = 1 \tag{2-47}$$

where ω_n is the denormalized upper passband edge, C_i is the integrator capacitor which is chosen arbitrarily for reasonable component values and R_i is the denormalizing resistance which is used to find R_{ij} with the equation:

$$R_{ij} = \frac{R_i}{A_{ij}} \tag{2-48}$$

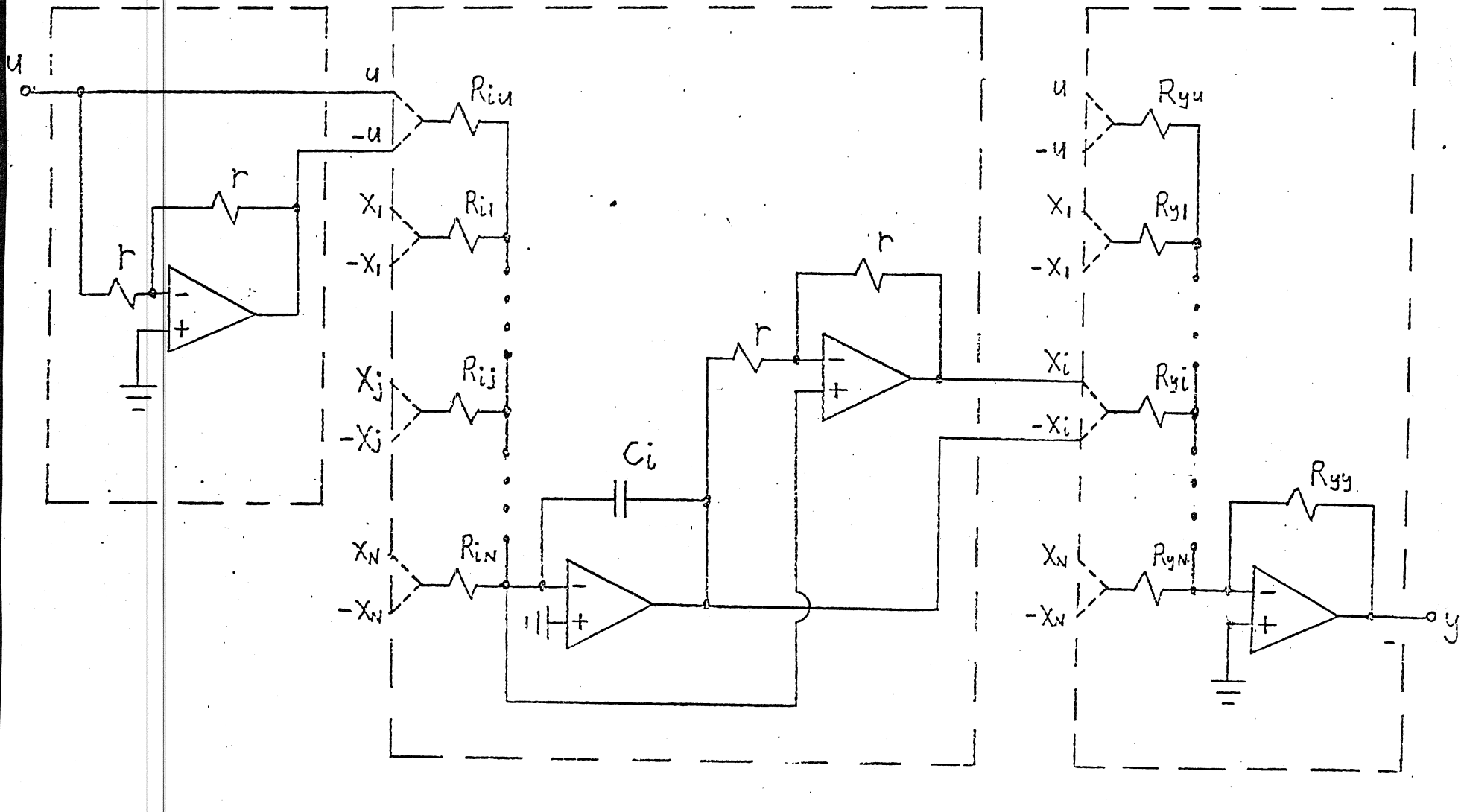

Figure 2.4 Circuit realization of a general state-space filter

The value of the feed-in resistor, R_{iu}, of integrator i is found from

$$R_{iu} = \frac{R_i}{b_i} \tag{2-49}$$

and the value of the resistors which sum the states together to form the output, R_{yi}, is found using

$$R_{yi} = \frac{R_{yy}}{c_i} \tag{2-50}$$

and the feed-through resistor, R_{yu}, is found with the equation

$$R_{yu} = \frac{R_{yy}}{d} \tag{2-51}$$

where the resistors R_{ij} and R_{yi} are connected to either positive or negative state, X_j or X_i, according to the sign of A_{ij} and c_i respectively. Similarly, the resistors R_{iu} and R_{yu} are connected to either the positive or negative input according to the sign of b_i and d respectively.

Note that if all the elements in a column of A and the corresponding column of c are negative then the inverting op-amp of that state is not required. It then follows that scaling by -1 can be used to minimize the number of op-amps in the final circuit.

The reason that the second op-amp has its positive input connected to the negative input of op-amp 1 is to obtain signal inversion without incurring any extra phase lag.

It can be seen from equation (2-48) that the the sensitivity of A_{ij} to R_{ij} is -1. Also from equations (2-49), (2-50), and (2-51) the sensitivities of b_i, c_i, and d to R_{iu}, R_{yi}, and R_{yu} respectively are all -1.

To find the sensitivity of γ_i with respect to the integrator capacitor, C_i, recall that

$$\gamma_i = \frac{1}{R_i C_i} \tag{2-52}$$

thus

$$S_{C_i}^{\gamma_i} = -1 \tag{2-53}$$

Now using

$$S_z^x = S_y^x S_z^y \tag{2-54}$$

we can write

$$S_{R_{ij}}^{T(s)} = S_{A_{ij}}^{T(s)} \cdot S_{R_{ij}}^{A_{ij}} \tag{2-55}$$

$$= g_i f_j \cdot \frac{A_{ij}}{T(s)} \cdot (-1) \tag{2-56}$$

Using this same method, the formulae for the sensitivity of $T(s)$ relative to the values of circuit elements can be found. The real part is then taken to obtain the following formulae for the magnitude of the sensitivities:

$$S_{R_{iu}}^{|T(s)|} = \mathrm{Re}\left[-g_i \cdot \frac{b_i}{T(s)}\right] \tag{2-57}$$

$$S_{R_{ij}}^{|T(s)|} = \mathrm{Re}\left[-g_i f_j \cdot \frac{A_{ij}}{T(s)}\right] \tag{2-58}$$

$$S_{R_{yu}}^{|T(s)|} = \mathrm{Re}\left[\frac{-d}{T(s)}\right] \tag{2-59}$$

$$S_{R_{yi}}^{|T(s)|} = \mathrm{Re}\left[-f_i \cdot \frac{c_i}{T(s)}\right] \tag{2-60}$$

$$S_{C_i}^{|T(s)|} = \mathrm{Re}\left[-f_i g_i \cdot \frac{s}{T(s)}\right] \tag{2-61}$$

A formula may also be derived to find the deviation of a transfer function as a result of changing the gain-bandwidth product of an op-amp in an integrator. Analysis of a Miller integrator gives the following formula

$$\frac{V_o}{V_i} = \frac{-1}{sC_i R_{eqi}\left[1+(\frac{1}{A})(1+\frac{1}{sC_i R_{eqi}})\right]} \tag{2-62}$$

where C_i is the integrator capacitance, R_{eqi} is the parallel equivalent of all feed-in resistances of integrator i and A is the finite op-amp gain of integrator i.

From the above equation we see that

$$\gamma_i = \frac{1}{C_i R_{eqi}\left[1+(\frac{1}{A})(1+\frac{1}{sC_i R_{eqi}})\right]} \tag{2-63}$$

which leads to

$$\frac{d\gamma_i}{d(\frac{1}{A})} = -C_i R_{eqi}\left[1+\frac{1}{sC_i R_{eqi}}\right]\cdot\gamma_i^2 \tag{2-64}$$

and since $\gamma_i \approx \frac{1}{C_i R_{eqi}}$

$$\frac{d\gamma_i}{d(\frac{1}{A})} = \frac{-1}{C_i R_{eqi}}\cdot\left[1+\frac{1}{sC_i R_{eqi}}\right] \tag{2-65}$$

It then follows that

$$\frac{dT(s)}{d(\frac{1}{A})}\cdot\frac{1}{T(s)} = S_{\gamma_i}^{T(s)}\cdot\frac{d\gamma_i}{d(\frac{1}{A})}\cdot\frac{1}{\gamma_i} \tag{2-66}$$

$$= S_{\gamma_i}^{T(s)}(-1)\left[1+\frac{1}{sC_i R_{eqi}}\right] \tag{2-67}$$

$$= -f_i g_i \frac{s}{T(s)} \left[1 + \frac{1}{sC_i R_{eqi}} \right] \tag{2-68}$$

Now assuming dominant pole compensation of the op-amps, we have

$$\Delta\left(\frac{1}{A}\right) \approx \frac{s}{\omega_t} - 0 = \frac{s}{\omega_t} \tag{2-69}$$

where ω_t is the op-amp unity-gain frequency in radians. The formula which gives the deviation of the transfer function resulting from a change in ω_t of the op-amp in integrator "i" is found from combining (2-68), (2-69), and taking the real part,

$$\frac{dT(s)}{T(s)} = -f_i g_i \frac{s}{T(s)} \left[1 + \frac{1}{sC_i R_{eqi}} \right] d\left[\frac{1}{A}\right] \tag{2-70}$$

$$d\ln|T(s)| + j d\varphi[T(s)] = -f_i g_i \frac{s^2}{\omega_t T(s)} \left[1 + \frac{1}{sC_i R_{eqi}} \right] \tag{2-71}$$

$$d\ln|T(s)| = \mathrm{Re}\left[-f_i g_i \frac{s^2}{\omega_t T(s)} \left[1 + \frac{1}{sC_i R_{eqi}} \right] \right] \tag{2-72}$$

$$\frac{\Delta|T(s)|}{|T(s)|} = -Re\left[f_i g_i \frac{s^2}{\omega_t T(s)} \left[1 + \frac{1}{sC_i R_{eqi}} \right] \right] \tag{2-73}$$

2.6 Dynamic Range

The dynamic range of a filter is determined by two limits. One limit occurs when the input signal level is large and the op-amps clip their output signals. The other limit occurs when the input signal level is small and the inherent noise in the op-amps becomes comparable to the signal level. After choosing the configuration of the filter, one then optimizes the dynamic range by ensuring that all op-amps will clip at approximately the same level of input signal. This optimization is done by scaling the intermediate-transfer functions, $\{f_i(s)\}$. To perform this scaling, one must first decide on a mathematical measure or norm for measuring the signal level at $X_i(s)$.

L_∞ scaling adjusts the filter so that if the input is a frequency swept sinusoid, then the output of each of the integrators will reach the same maximum value. An L_∞ norm is defined as:

$$\|f_i\|_\infty = MAX\ |f_i(j\omega)| \quad (\omega_1<\omega<\omega_2) \tag{2-74}$$

where ω_1 and ω_2 define the frequency band of interest.

L_2 scaling adjusts the filter so that if the input is white noise then the output of each of the integrators will have the same RMS value. An L_2 norm is defined as:

$$\|f_i\|_2 = \sqrt{\int_{-\infty}^{\infty} |f_i(j\omega)|^2 d\omega} \tag{2-75}$$

No matter which norm is chosen, L_p scaling is accomplished by choosing all factors, α_i, such that for the scaled filter

$$\|f_i\|_p = \frac{M}{M_u} \quad , \text{for all } i \tag{2-76}$$

where M is the maximum allowable output voltage of each op-amp and M_u is the maximum input voltage measured using an L_p norm. When using a norm other than L_∞, one should refer to [1] to see how one can determine M.

Once scaling has been performed on a filter then its dynamic range can be simply measured by the amount of its output noise. The output noise of the filter results from the inherent noise of the op-amps and is measured with the filter input grounded. This output noise changes from structure to structure and is determined by the set of functions, $\{g_i(s)\}$.

If one assumes that the integrators have independent white input noise of equal power then the noise gain, $N_o(\omega)$, of the filter is

$$N_o(\omega) = \sum_{i=1}^{N} |g_i(j\omega)|^2 \tag{2-77}$$

One can look at the total noise contributions of the individual integrators using the formula

$$N_i = \|g_i\|_2 \tag{2-78}$$

$$= \int_{-\infty}^{\infty} |g_i(j\omega)|^2 d\omega \tag{2-79}$$

Then the total output noise, N_{tot}, resulting from all the integrators together is simply

$$N_{tot} = \sum_{i=1}^{N} N_i \tag{2-80}$$

assuming each integrator has independent white input noise with a spectral density of 1 $V^2/(rad/sec)$.

An N x N matrix, **K**, which assists in finding the L_2 norms of $\{f_i\}$ is defined in [9] as

$$K_{ij} = f_i \cdot f_j = \int_{-\infty}^{\infty} \overline{f_i(j\omega)} f_j(j\omega) d\omega \tag{2-81}$$

so that

$$K_{ii} = \left[\|f_i\|_2\right]^2 \tag{2-82}$$

Another N x N matrix, **W**, which helps to find the L_2 norms of $\{g_i\}$ is also defined as

$$W_{ij} = g_i \cdot g_j = \int_{\omega} \overline{g_i(j\omega)} g_j(j\omega) d\omega \tag{2-83}$$

so that

$$W_{ii} = \left[\|g_i\|_2\right]^2 \tag{2-84}$$

To compute the matrices K and W, a hermitian N x N matrix Q is defined as [1]

$$Q_{ij} = \frac{-2\pi}{\overline{e_i} + e_j} \tag{2-85}$$

where e_i is the i'th natural mode as defined in section 2.2.

The K and W matrices are then

$$K = \overline{F} Q F^T \tag{2-86}$$

$$W = \overline{G} Q G^T \tag{2-87}$$

2.7 Conclusions

This chapter presented tools needed in the design and analysis of state-space filters. The next chapter will show that filter analysis using formulae presented here agree closely with experimental measurements. Most of these

formulae are general and are valid for any state-space structure.

Using the material of this chapter as a basis, one can analyze a particular state-space filter so that its performance may be compared against that of other realizations of the particular filter. A question which still requires answering is how to find a "good" state-space realization without using an exhaustive search. In the following chapters, an attempt is made to provide an answer.

3. EXPERIMENTAL VERIFICATION

State space filter realizations have been investigated here at the University of Toronto for a few years, yet practically all the comparisons between different state-space filters have been through computer simulations. In this chapter, we present experimental verification for the sensitivity and dynamic range relationships of state-space systems. Also shown are a number of sensitivity comparisons between existing methods of ladder simulation and a state-space design.

3.1 Description of Filter Examples

An eighth order bandpass filter was designed and constructed and experimental results compared to theoretical predictions. The filter's passband extends from 1 kHz to 1.4 kHz with .4 dB ripple. The stopband's required attenuation is 50 dB below 700 Hz and above 1700 Hz. The filter was frequency normalized so that the upper passband edge (1400 Hz) was at 1 rad/s. Unless otherwise stated all results will be frequency normalized. The transfer function polynomials satisfying the above constraints are shown in Table 1 below. A passive LC ladder realization which is also frequency normalized is shown in Figure 3.1.

A number of state-space filters with different dynamic range and sensitivity properties can simulate the workings of the above LC ladder. Experimental

Polynomial	natural mode	loss pole	reflection zero
Leading Coeff.	1210.19	5.31423	3896.19
Roots	-0.068135±j0.916348	0	±j0.909524
	-0.068805±j0.788556	0	±j0.989195
	-0.023287±j0.710193	±j1.25008	±j0.796951
	-0.026288±j1.004480	±j0.39973	±j0.723908

TABLE 1. Transfer Function

measurements were made on a state-space filter which was derived from a "good ladder simulation" from the doctoral thesis of Martin Snelgrove [1]. This "good" filter simulated all the capacitor voltages and inductor currents of the above ladder except for V_{C_3} and V_{C_6}. The reasoning for this choice of elements simulated will become more apparent after reading chapter 4 of this thesis. The filter was scaled for optimum dynamic range using an L_2 norm as explained in chapter 2 of this thesis. The scaling was done so that all $\|f_i\|=1$ and the filter was designed for a unity passband gain.

The resulting state-space system is:

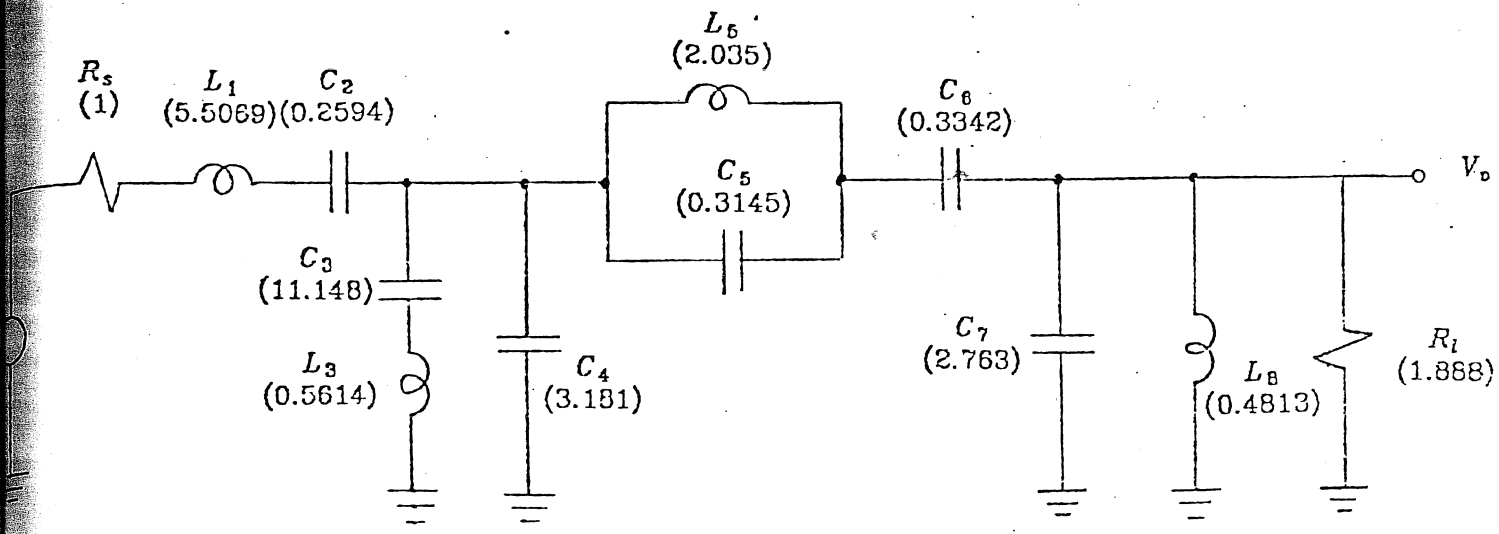

Figure 3.1 Eighth order bandpass LC ladder

$$\mathbf{A}=\begin{vmatrix} -0.1816 & 0 & 0.8288 & 0 & 0 & 0.1801 & 0 & 0 \\ 0 & 0 & -0.0695 & -0.0465 & 0 & 0.8533 & -0.0164 & 0 \\ -0.8445 & 0 & 0 & 0 & 0 & 0 & 0 & 0 \\ -0.0615 & -0.1675 & 0 & 0 & 0.9235 & 0 & 0.0313 & 0.1459 \\ 0 & 0 & 0 & -0.9065 & 0 & 0 & 0 & 0 \\ -0.3023 & -0.8235 & 0 & 0 & 0.1893 & 0 & -0.0074 & -0.0345 \\ -0.0199 & -0.0542 & 0 & 0 & -0.2589 & 0 & -0.1816 & -0.8454 \\ 0 & 0 & 0 & 0 & 0 & 0 & 0.8426 & 0 \end{vmatrix} \quad \mathbf{b}=\begin{vmatrix} -0.2814 \\ 0 \\ 0 \\ 0 \\ 0 \\ 0 \\ 0 \\ 0 \end{vmatrix}$$

$$\mathbf{c}^T = \begin{bmatrix} 0 & 0 & 0 & 0 & 0 & 0 & 0.7848 & 0 \end{bmatrix} \qquad d = 0$$

To get minimum op-amp count, f_3 and f_5 were scaled by -1 so that columns 1, 2, and 4 have only negative elements.

The filter built uses type LF356H op-amps which have a gain-bandwidth product of 3 MHz. All the component values were chosen to within .1 percent of their nominal value. Figure 3.2 shows the predicted and measured transfer function response of the filter.

Also designed and built was a third order elliptic low-pass state-space filter. The passband edge is at 1 kHz but as before all results will be normalized so that the upper passband edge is at 1 rad/s. Thus, the normalized filter has a passband from 0 rad/s to 1 rad/s with a ripple of 1 dB. Its stopband is from 1.4 rad/s to ∞ with a minimum attenuation of 22 dB. A transfer function which satisfies the above specifications has a loss pole at ∞ and a pair of loss poles at $\pm j1.5536$. The transfer function has a pair of poles at $-0.17607 \pm j0.99853$ and one pole at -0.61342. An LC ladder implementing this transfer function is shown in figure 3.3.

A state-space filter was designed to simulate the ladder of figure 3.3 where the chosen states are V_{C_1}, I_{L_2}, and V_{C_3}. The filter was then scaled for dynamic range using L_∞ scaling. The resulting state-space system is

$$\mathbf{A} = \begin{bmatrix} -0.4828 & -0.4505 & -0.0961 \\ 1.1410 & 0 & -0.8390 \\ -0.1777 & 0.6127 & -0.4828 \end{bmatrix} \qquad \mathbf{b} = \begin{bmatrix} 0.7100 \\ 0 \\ 0.2613 \end{bmatrix}$$

$$\mathbf{c}^T = \begin{bmatrix} 0 \\ 0 \\ 1 \end{bmatrix} \qquad d = 0$$

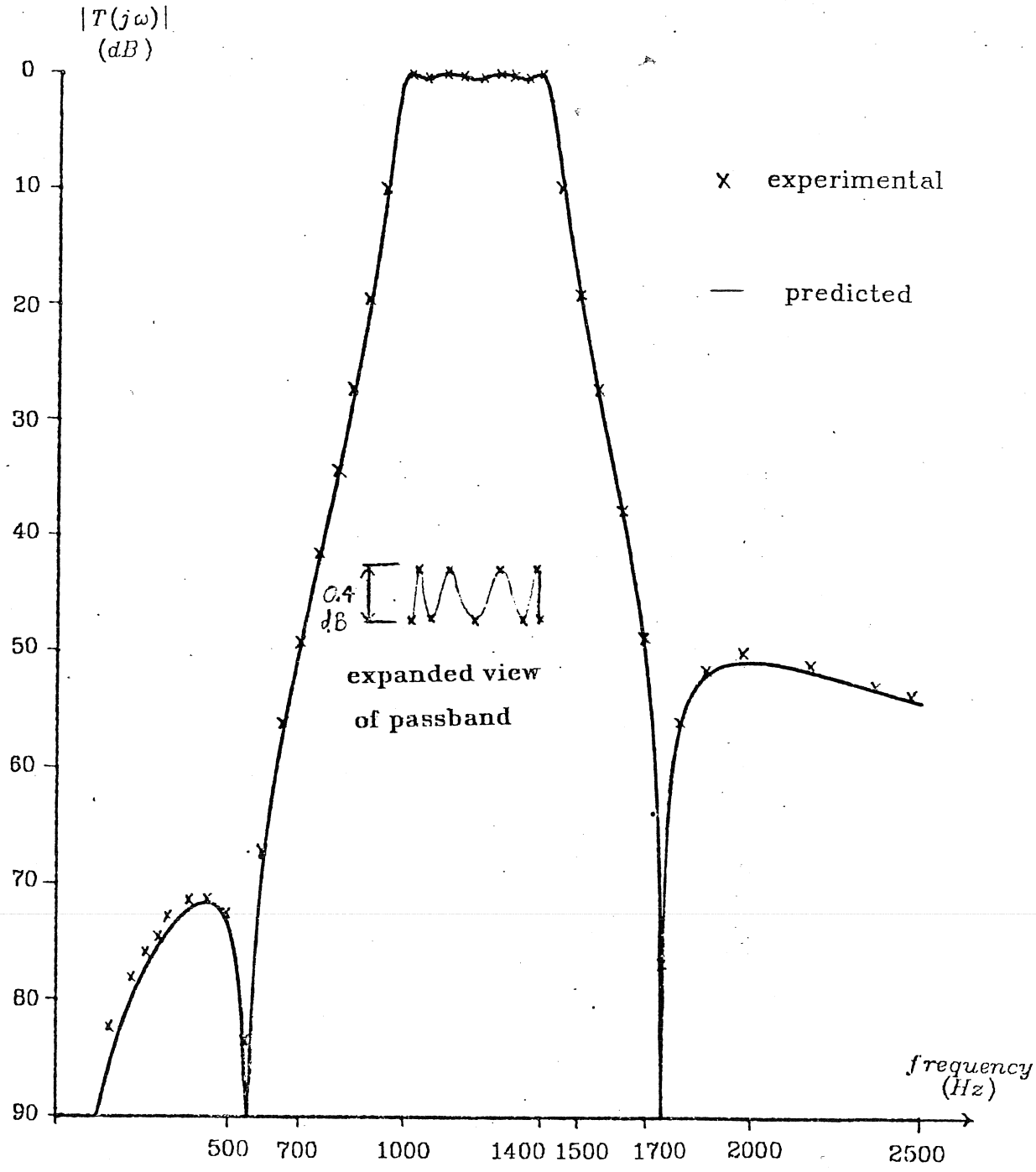

Figure 3.2 Eighth order transfer function

(Experimental vs. Predicted)

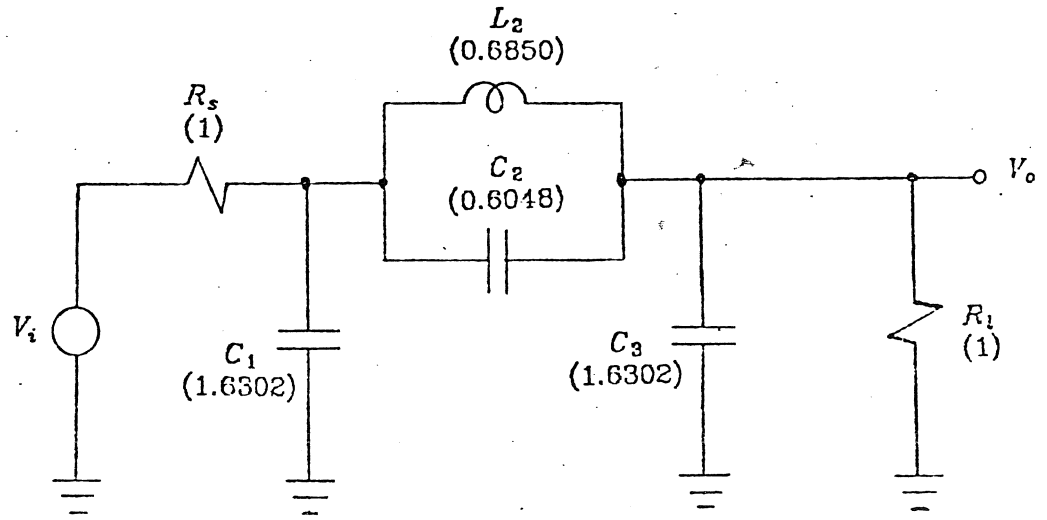

Figure 3.3 Third Order lowpass LC ladder

3.2 Resistor Sensitivity

Resistor sensitivity was measured by changing a resistor by 5 percent then comparing the perturbed transfer function with the predicted transfer function. The sensitivity of resistor R_{ij} is directly proportional to A_{ij} so usually the largest A_{ij} in magnitude corresponds to the resistor with the greatest sensitivity. Since A_{45} is the largest element in the A matrix of the eighth order filter, R_{45} was changed to observe it's sensitivity. The predicted and measured resistor sensitivity results are shown in figure 3.4.

Resistor R_{42}, of the eighth order filter, was also varied to compare its predicted and measured sensitivities. The results are shown in figure 3.5.

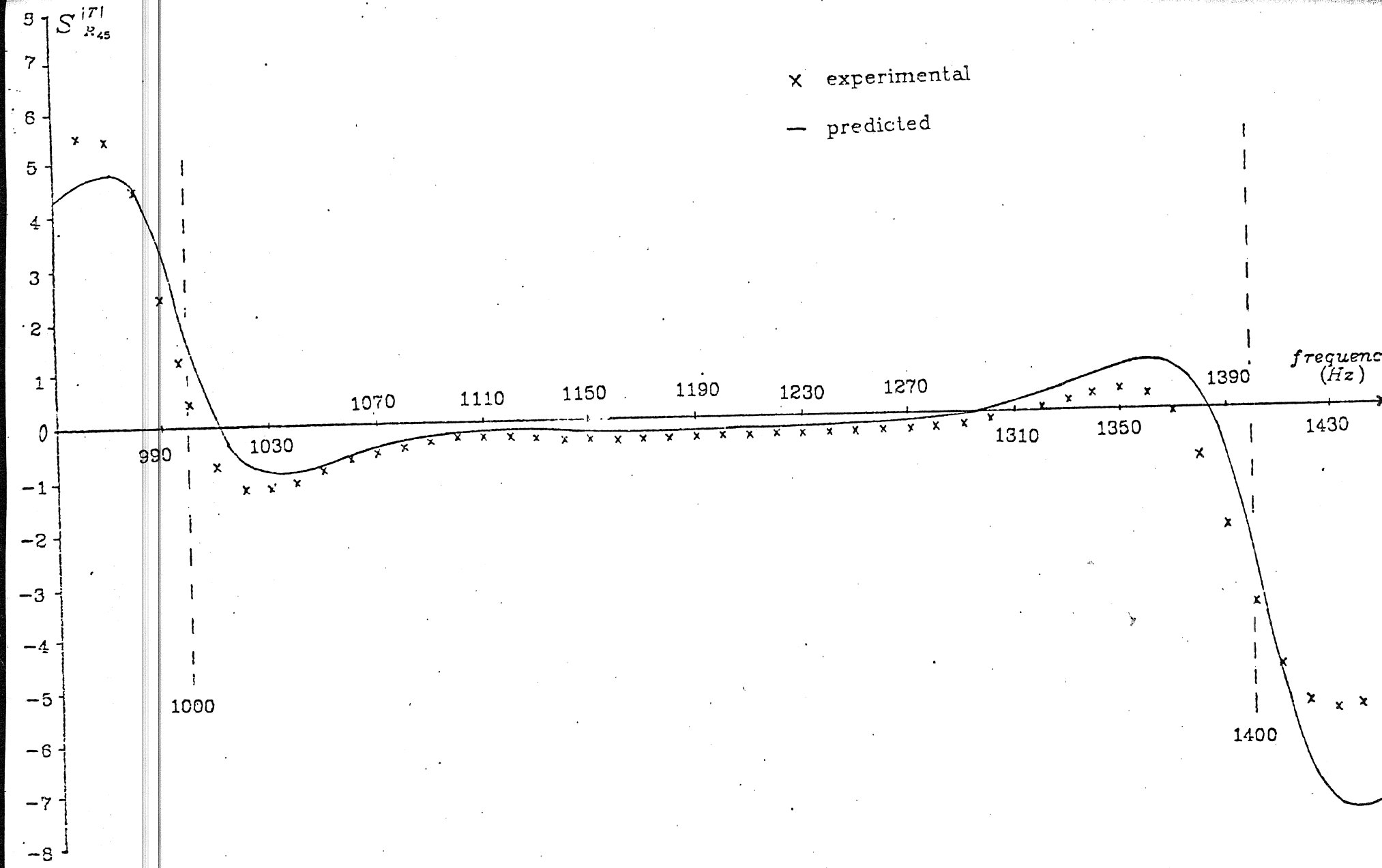

Figure 3.4 Sensitivity resulting from a 5 percent deviation in R_{45} of the eighth order filter

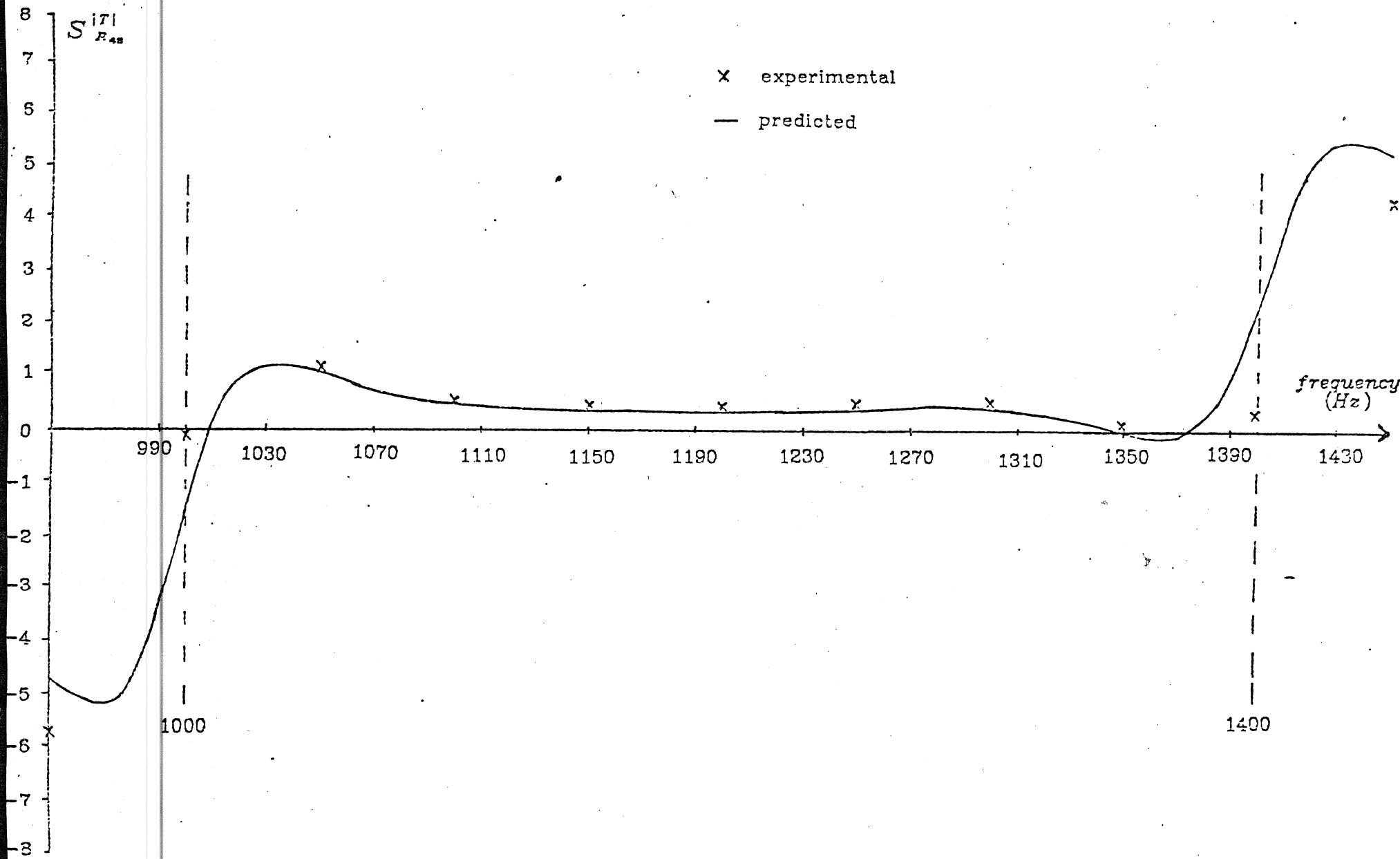

Figure 3.5 Sensitivity resulting from a 5 percent deviation in R_{42} of the eighth order filter

For the third order low-pass filter, resistor R_{21} was varied to compare predicted and measured sensitivities. The results are shown in figure 3.6.

As seen from the comparisons of predicted and experimental results, resistor sensitivities are very accurately predicted.

3.3 Integrator Sensitivity

Evaluating the integrator sensitivity formula using the computer, it was predicted that the eighth-order filter was most sensitive relative to the gain of integrator number 4. To compare predicted and measured integrator-gain sensitivity, the op-amp of integrator 4 was substituted with a type 741 op-amp having a measured unity-gain frequency of 600 kHz. Recalling equation (2-73), note that it is derived assuming an ideal integrator is substituted with a real integrator using an op-amp of gain-bandwidth product ω_t. In this measurement we are actually substituting an op-amp of unity-gain frequency of 3 MHz with another op-amp of unity-gain frequency of 600 kHz. To a first order effect, this can be accounted for by subtracting the deviation in the transfer function corresponding to a 3 MHz op-amp from the deviation corresponding to a 600 kHz op-amp. This, in turn, is equivalent to changing an ideal integrator to one using an op-amp with a gain-bandwidth product of

$$\left[\frac{1}{600\ kHz} - \frac{1}{3\ MHz}\right]^{-1} = 750\ kHz \qquad (3\text{-}1)$$

So equation (2-35) is used with ω_t equal to $(2\pi)750\ rad/s$ which is then

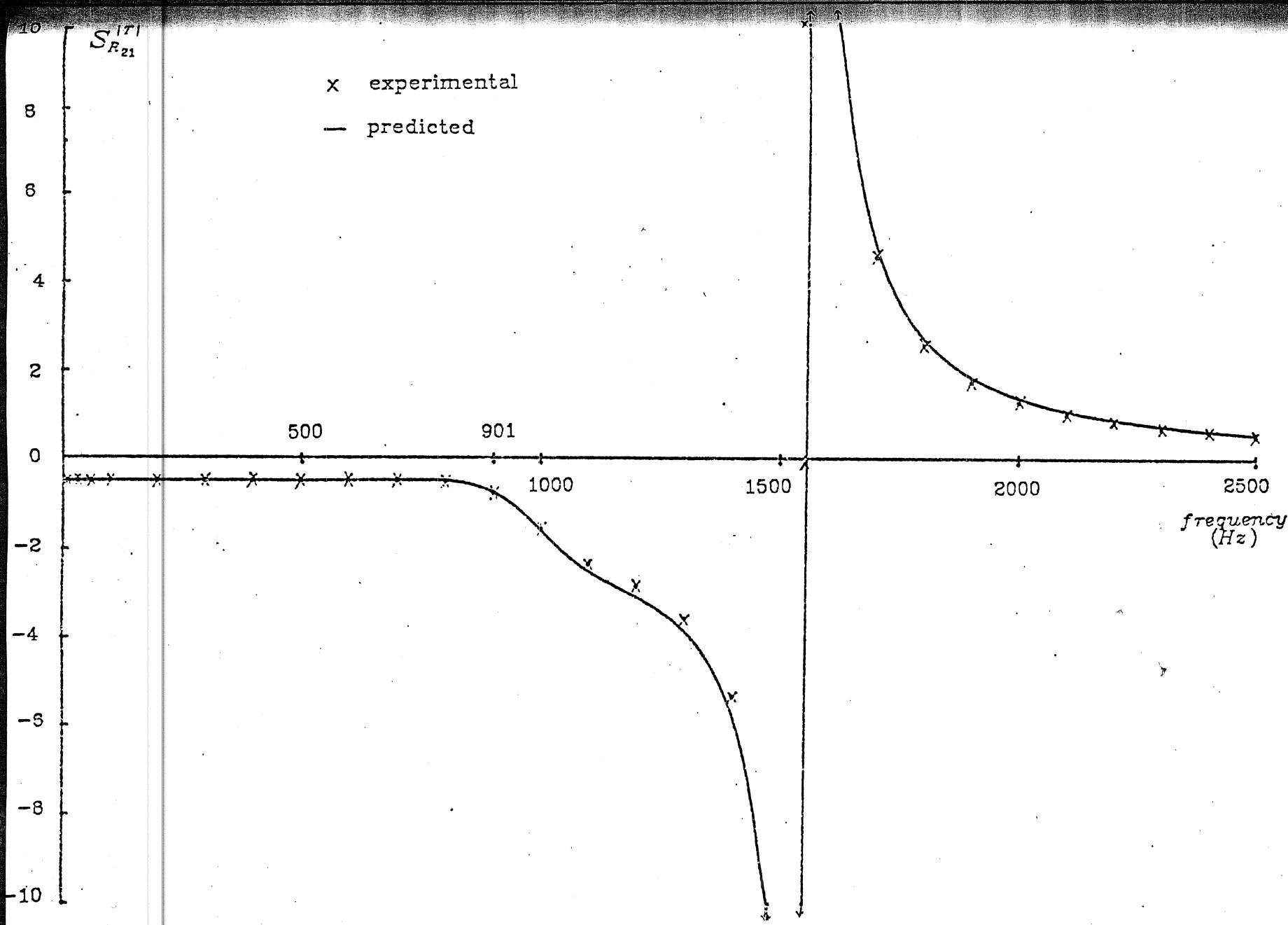

Figure 3.6 Sensitivity resulting from a 5 percent deviation in R_{21} of the third order filter. Note that the plot is truncated at ± 10.

normalized using 1400 Hz.

The predicted and measured results are shown in figure 3.7. These results show that the effects of the finite op-amp gain can be accurately predicted.

3.4 Dynamic Range

Typically, filters of a given structure are easily scaled for optimum dynamic range. The output of each op-amp is adjusted so that all op-amps will saturate at approximately the same level of input signal. What then determines the dynamic range of an active RC filter is the output noise of the filter (which changes from structure to structure) resulting from inherent op-amp noise.

The output noise voltage of a state-space filter can be predicted using equation (2-77) and the input noise voltage of the op-amps used. Figure 3.8 shows the predicted noise gain, in dB, of the eighth order filter described above. The right-hand scale, of the same figure, shows the output noise voltage level in dB using the reference 1 volt RMS to be 0 dB. This scale was obtained assuming that the op-amps input noise are white with $12\,nV/\sqrt{Hz}$ density, which is the noise specification for the type LF356 used in the experiment. The scale is also adjusted to account for the spectrum analyzer having a resolution bandwidth of 3 Hz.

Figure 3.9(a) shows the actual output noise voltage measured for the eighth order filter with the input grounded. The resolution bandwidth of the spectrum analyzer was 3 Hz. An expanded view of the passband noise is shown in figure

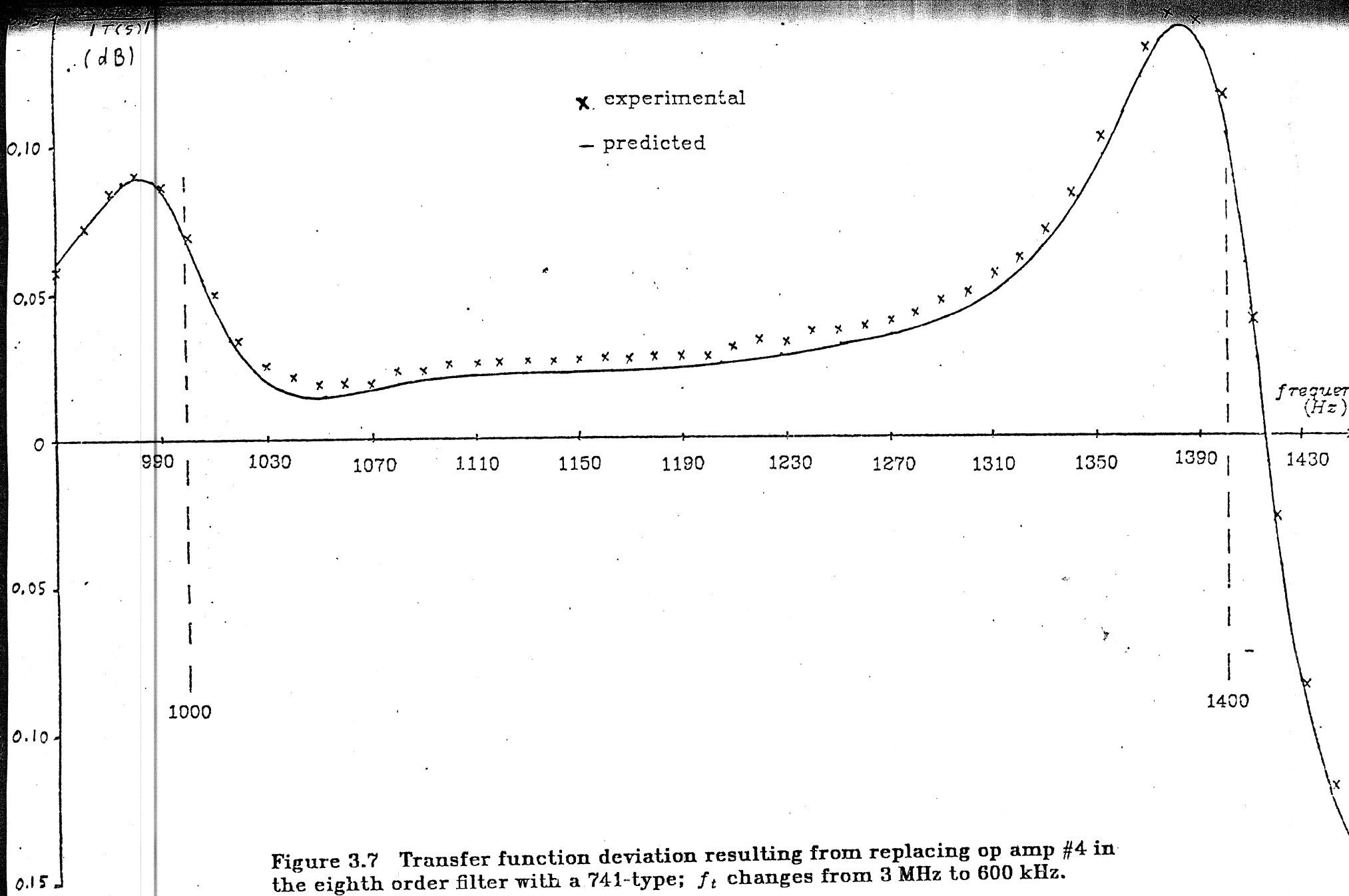

Figure 3.7 Transfer function deviation resulting from replacing op amp #4 in the eighth order filter with a 741-type; f_t changes from 3 MHz to 600 kHz.

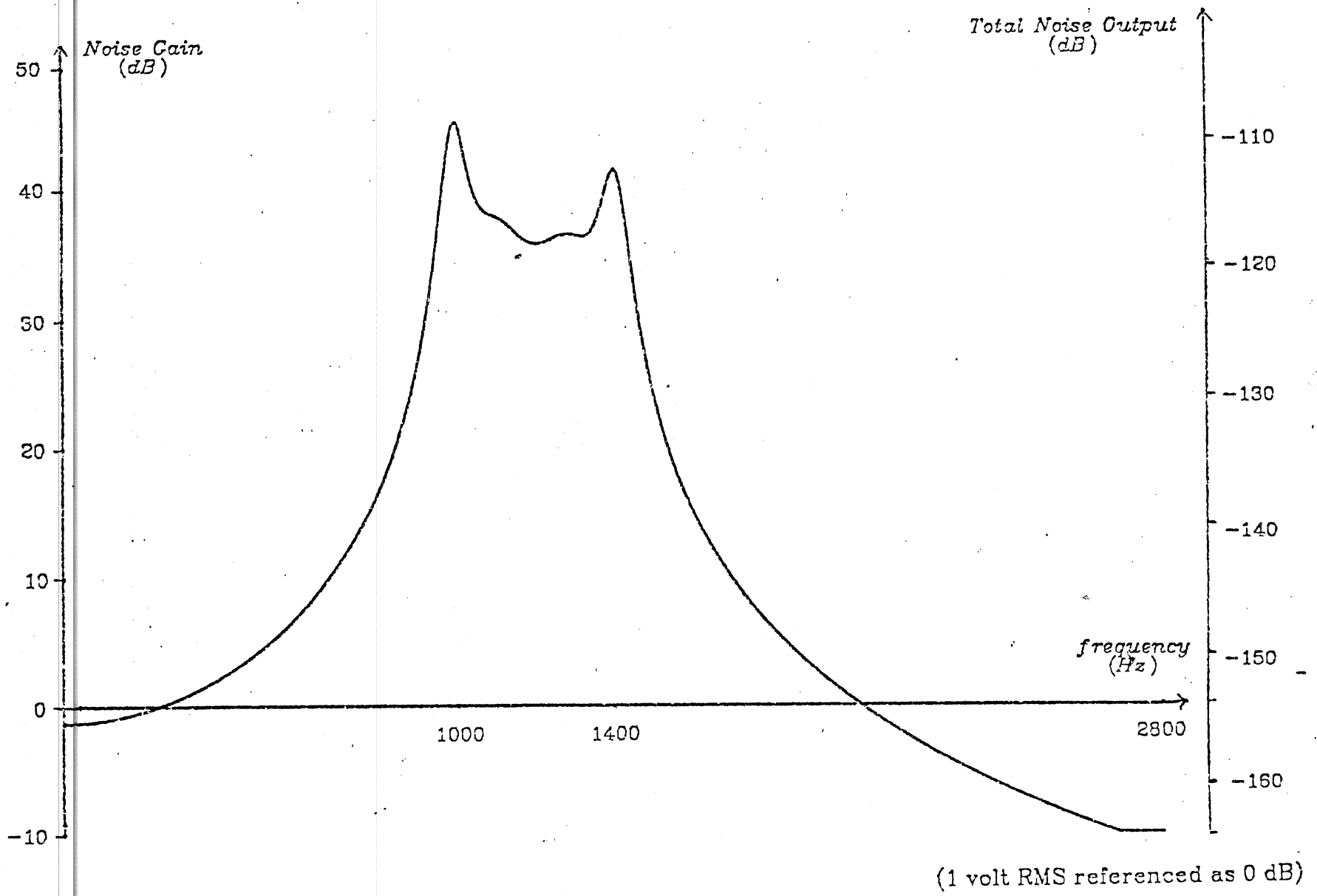

Figure 3.8 Predicted noise for the eighth order filter

3.9(b).

The predicted and measured output noise voltage of this filter agree remarkably well for noise results!

3.5 Sensitivity Comparisons

In order to convey to the reader a feeling on how good the sensitivity of state-space filters is, comparisons between state-space filters and two existing methods of ladder simulations will be shown.

3.5.1 Capacitor Splitting

The third order low-pass LC ladder of figure 3.3 was used to design two active RC filter simulations. One is the third order state-space filter (L_∞ scaled circuit shown in figure 3.10) described above. The other design is described below.

A commonly used method to simulate this ladder is to take capacitor C_2 and split it as shown in figure 3.11(a), which maintains the transfer function of the filter unchanged. One then uses Norton's theorem to obtain the equivalent circuit shown in figure 3.11(b). A node equation is written at both V_1 and V_3 and a loop equation is written for the loop containing the two capacitors and the inductor yielding

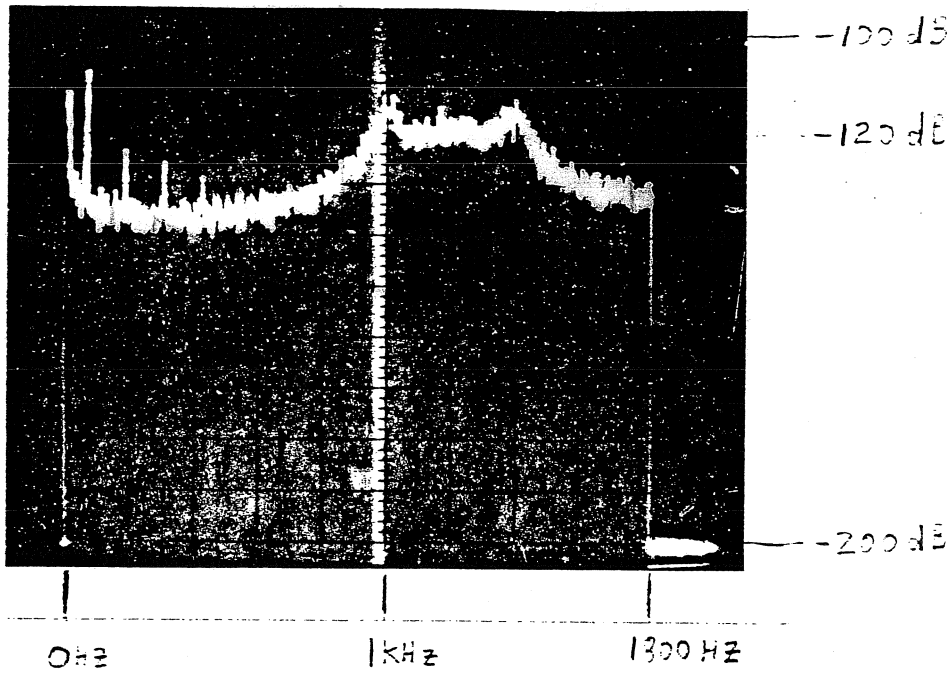

(a) Horizontal: 200 Hz/div.
Vertical: 10 dB/div.
Resolution Bandwidth: 3 Hz

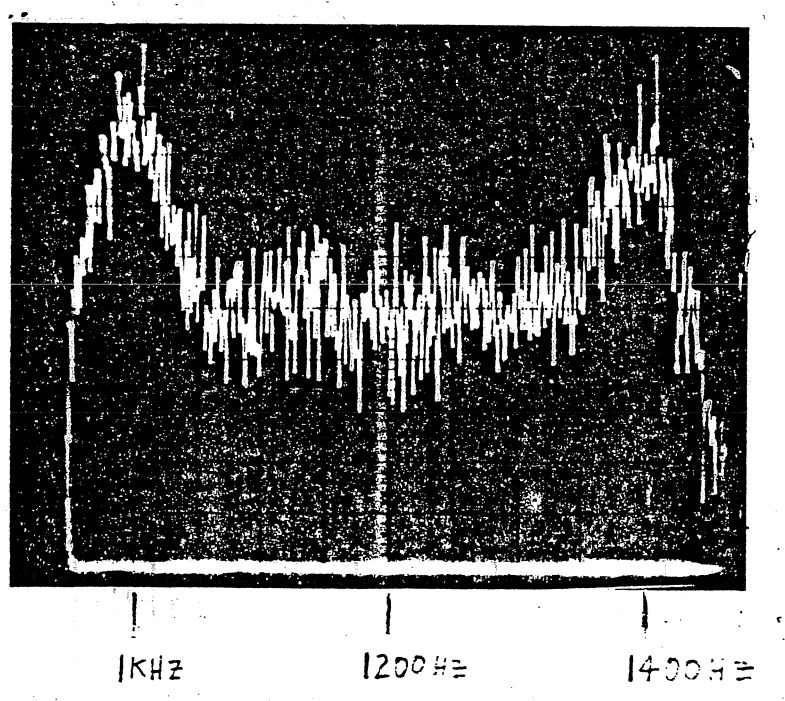

(b) Horizontal: 50 Hz/div.
Vertical: 1 dB/div.
Resolution Bandwidth: 10 Hz

Figure 3.9 Measured output noise voltage for the eighth order filter

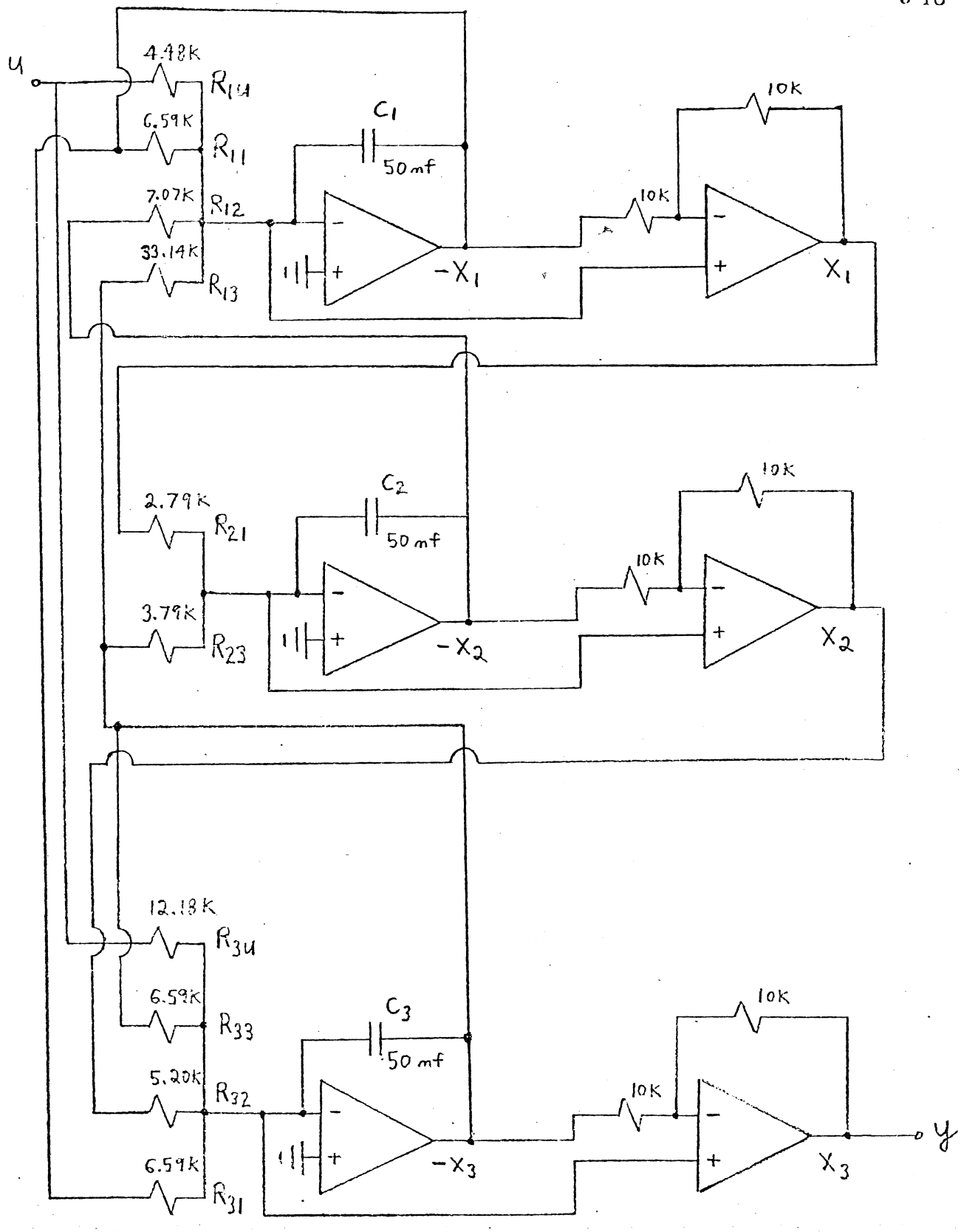

Figure 3.10 Circuit implementation of the third order state-space filter

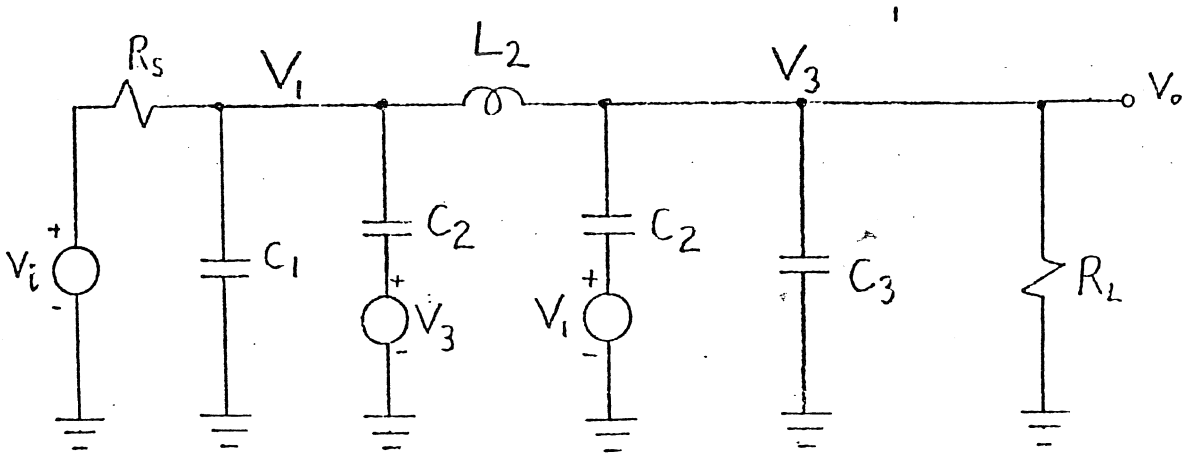

(a)

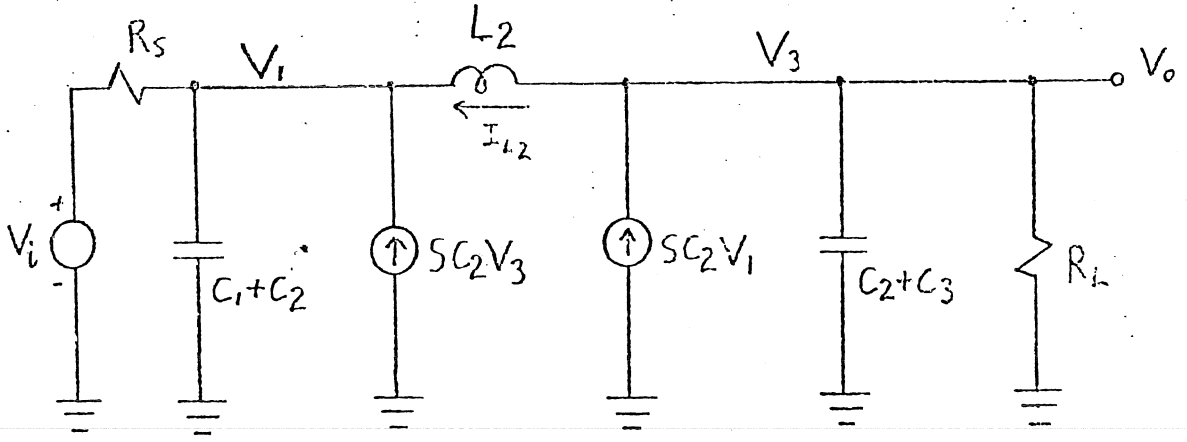

(b)

Figure 3.11 Circuit manipulations for the capacitor-splitting technique of ladder simulation

$$s(C_1+C_2)V_1 = \frac{1}{R_s}(V_i-V_1)+I_{L_2}+sC_3V_3 \tag{3-2}$$

$$s(C_2+C_3)V_3 = \frac{-1}{R_l}(V_3)-I_{L_2}+sC_2V_1 \tag{3-3}$$

$$sL_2I_{L_2} = V_3-V_1 \tag{3-4}$$

Note that if we consider V_1, V_3, and I_{L_2} to be states then the right hand side of the above equations are inputs to the integrators which form the states. The inputs sC_2V_3 and sC_2V_1 are capacitor inputs to the integrators forming V_1 and V_3. The resulting filter is a non-canonic realization of the transfer function and is known to have good sensitivity properties. The filter was scaled using L_∞ scaling and its circuit implementation is shown in figure 3.12.

Figure 3.13 shows the experimentally measured maximum sensitivity results relative to integrator input elements versus frequency of the two filters. It is seen that the state-space filter performs slightly better at higher frequencies. Though the sensitivity results of these two filters are approximately the same, it is important to note that the capacitor splitting technique presently has no method of predicting these results. Also, the capacitor splitting technique is limited in use. The technique can be used on LC ladders to eliminate the problem of capacitive tiesets and a modified version of the technique can also deal with the problem of inductive cutsets, yet presently, the technique has no method of dealing with capacitor cutsets or inductive tiesets in ladders.

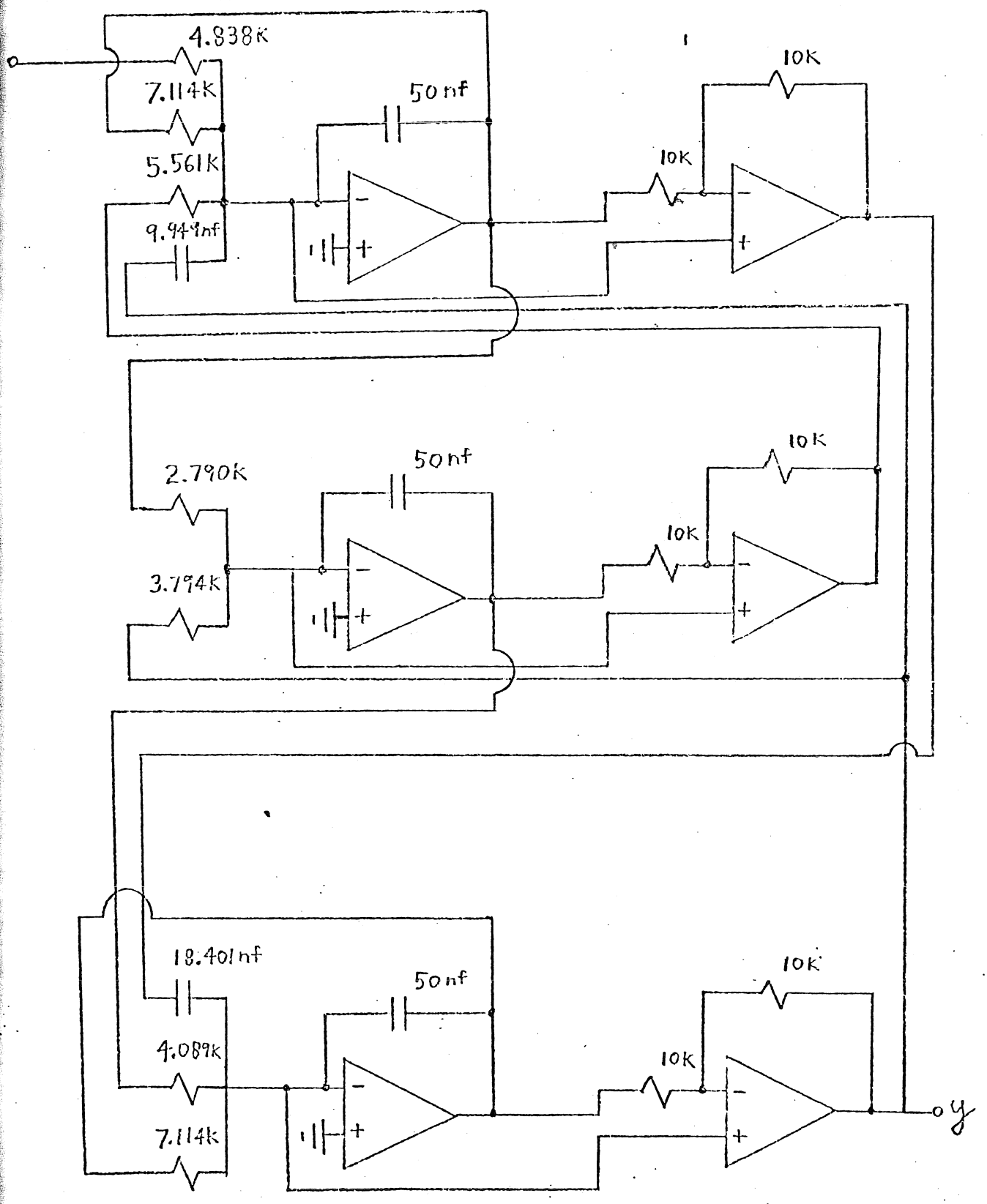

Figure 3.12 Circuit implementation for the third order filter, obtained using the capacitor-splitting technique

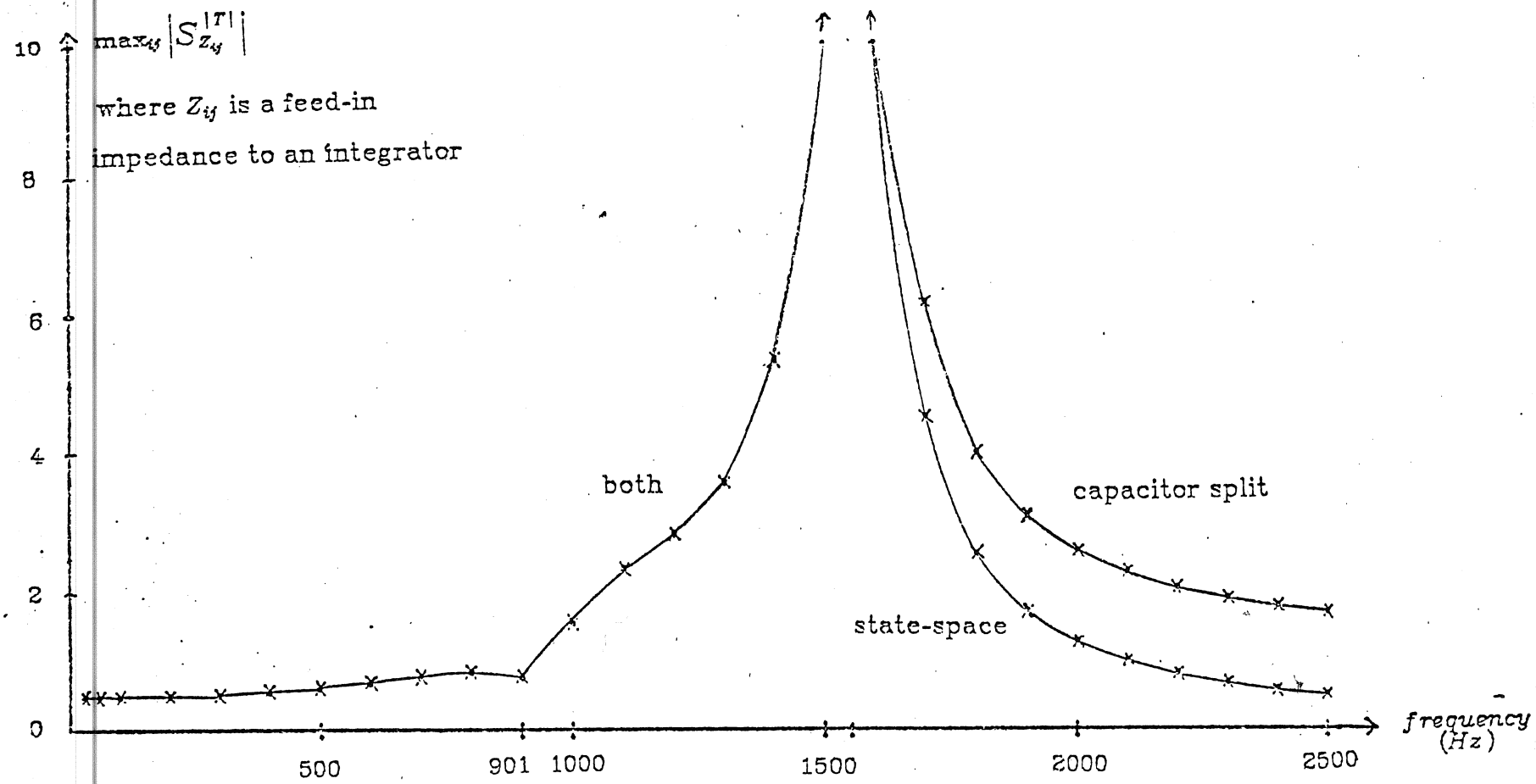

Figure 3.13 Experimental sensitivity comparison between capacitor-split and state-space filters

3.5.2 Signal Flow Graph (SFG) Filters

A twelfth order LC ladder is shown in figure 3.14. This filter was actively simulated using signal flow graph (SFG) techniques by Ken Martin [5]. The resulting active filter required 25 op-amps and the most sensitive element had a measured sensitivity figure of 4.1 at the most critical frequency.

Using the computer program dot [10], to design a state-space filter from the ladder of figure 3.14, sensitivity figures for the resistors can be predicted as shown above. All inductor currents and capacitor voltages were chosen as states except for V_{C_3}, V_{C_5}, V_{C_7}, and V_{C_9}. The resulting state-space system is

$$
\mathbf{A}=\begin{vmatrix}
-0.1000 & -0.9275 & -0.0803 & 0 & 0.0353 & 0 & 0.0116 & 0 & 0 & 0 & 0 & 0 \\
0.9284 & 0 & 0 & 0 & 0 & 0 & 0 & 0 & 0 & 0 & 0 & 0 \\
0.8339 & 0 & 0 & -1.1676 & 0 & 0 & 0 & 0 & 0 & 0 & 0 & 0 \\
-0.0623 & -0.5845 & 0.7489 & 0 & 0.0690 & 0 & 0.0234 & 0 & 0 & 0 & 0 & 0 \\
0 & 0 & 0 & -0.4989 & 0 & 1.0191 & 0 & 0.3846 & 0 & 0 & 0 & 0 \\
-0.0219 & -0.2055 & 0.2634 & 0 & -0.7462 & 0 & -0.2493 & 0 & 0.0862 & 0 & 0 & -0.0171 \\
0 & 0 & 0 & 0 & 0 & 0.2880 & 0 & -0.8309 & 0 & -0.2398 & 0 & 0 \\
0 & -0.0868 & 0.1112 & 0 & -0.3152 & 0 & 0.8450 & 0 & -0.2910 & 0 & 0 & 0.0599 \\
0 & 0 & 0 & 0 & 0 & 0 & 0 & 0.2928 & 0 & -0.9028 & -0.2670 & 0 \\
0 & -0.0191 & 0.0244 & 0 & -0.0691 & 0 & 0.1854 & 0 & 0.8669 & 0 & 0 & -0.1783 \\
0 & 0 & 0 & 0 & -0.0101 & 0 & 0.0272 & 0 & 0.1270 & 0 & 0 & 0.9306 \\
0 & 0 & 0 & 0 & 0 & 0 & 0 & 0 & 0 & 0 & -0.9360 & -0.1002
\end{vmatrix}
$$

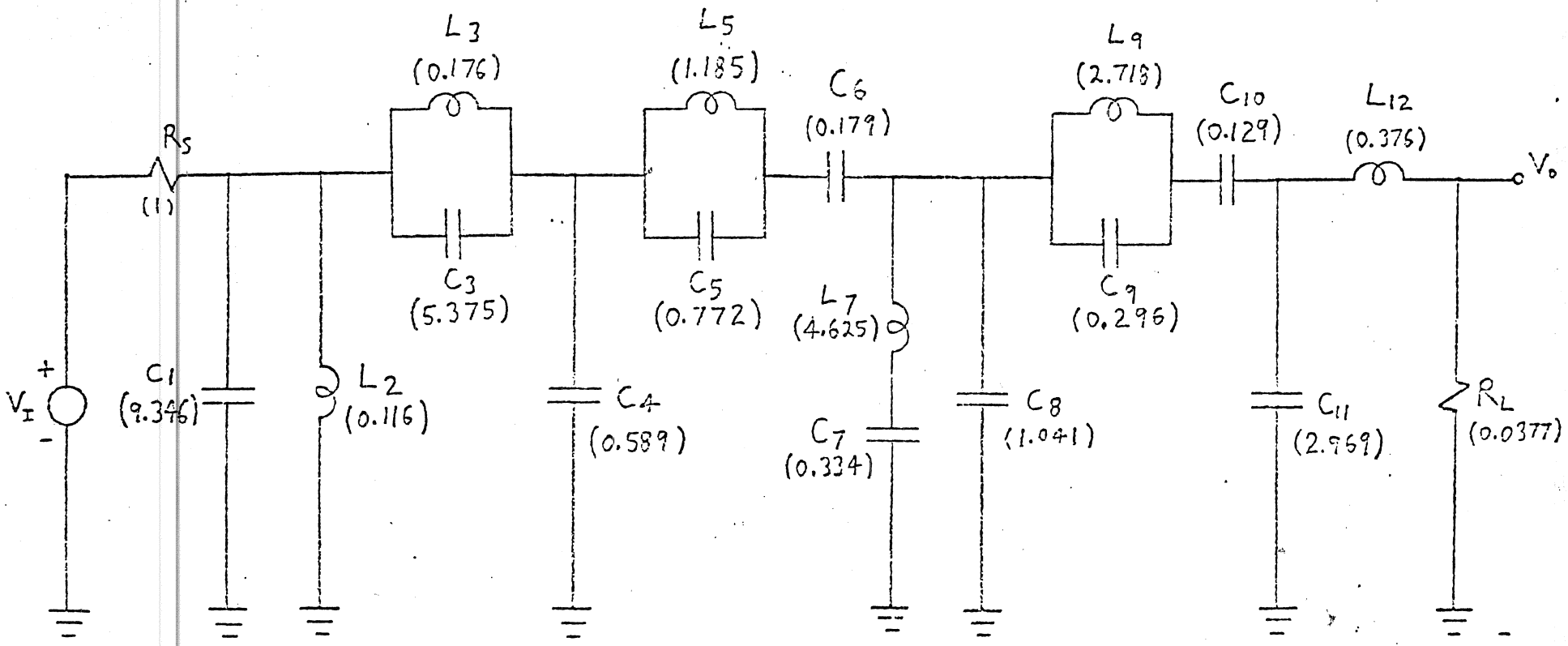

Figure 3.14 A twelfth order LC ladder

$$\mathbf{b}^T = \begin{bmatrix} 0.2030 & 0 & 0 & 0.1279 & 0 & 0.0450 & 0 & 0.0190 & 0 & 0 & 0 & 0 \end{bmatrix}$$

$$\mathbf{c}^T = \begin{bmatrix} 0 & 0 & 0 & 0 & 0 & 0 & 0 & 0 & 0 & 0 & 0 & -0.5335 \end{bmatrix} \quad d = 0$$

The predicted maximum sensitivity figure for any of the integrator input resistors is 5.7 at its most sensitive frequency. This indicates that the sensitivities of the two filter implementations are approximately the same considering that this is a first order prediction and the SFG sensitivity figure is a measured value. As well, a cascade design was tested in [5] and gave a sensitivity figure of 70 for the most critical element.

The number of op-amps required to build this twelfth order state-space filter is 20. We obtain this number by observing that 4 columns in the system description have only negative entries. As well, all the **b** and **c** elements are of the same sign. Since only one op-amp will be needed for each column consisting of only negative numbers then the total number of op-amps is simply $4 + (2 \times 8) = 20$. No op-amps are required for the input and output stages since all the elements in **b** and **c** are of the same sign. Thus this implementation provides a saving of 5 op-amps as compared to the SFG design.

As well, the SFG method requires reciprocators which are typically difficult to compensate and add high frequency noise to the final filter.

3.6 Conclusions

All of the above experimental results show that the sensitivity and dynamic range of state-space filters are accurately and easily predicted using the formulae of chapter 2. This combined with the low sensitivity values of state-space filters give this filter design method a distinct advantage over any existing method of LC ladder simulation.

In the remainder of this thesis, we will be concerned with presenting a direct and simple method to design state-space filters which simulate arbitrary LC ladders.

4. Choosing Ladder States to Simulate

One can simulate an N'th-order LC ladder by having the outputs of N integrators connected in a state-space configuration emulate the capacitor voltages and inductor currents of the ladder. In a canonic N'th order LC ladder, the total number of inductors and capacitors equals the order, N. So for a canonic state-space system to simulate an N'th order canonic ladder, the N states emulated are all the capacitor voltages and inductor currents of the ladder. In simpler terms, the transfer function from the input voltage to a capacitor voltage or inductor current of the LC ladder is the same as the transfer function from the input voltage of the active filter to the integrator output which emulates that element's voltage or current. If an element's voltage or current transfer function is the same in the LC ladder as an integrator output transfer function in the state-space filter, then we say that the element's voltage or current was chosen as a state for the state-space filter.

For a canonic simulation of a non-canonic N'th order LC ladder, only N states are chosen though there are more than N inductors and capacitors. It is important which N states are chosen as the resulting filter can have poor sensitivity and dynamic range properties or, perhaps, not even be realizable. In this chapter, we will give some insight as to which states should be chosen for a given LC ladder, and present a simple rule-of-thumb to simplify the choice.

4.1 Method of Sensitivity Comparison

It was shown in [1] that the optimum (though not necessarily obtainable) filter, with respect to integrator sensitivity, for a particular N'th order transfer function, $T(s)$, will have its integrator sensitivity as

$$optimum\ S_{\gamma_i}^{T(s)} = -\frac{s}{NT(s)}\frac{dT(s)}{ds} \quad , \text{for } all\ i \tag{4-1}$$

This optimum filter is called a Frequency Scaled Lower Bound (FSLB) filter.

Then as a method of plotting the integrator sensitivity of a filter, we can gain more insight if we plot a function which is proportional to the sensitivity magnitude, $\left|S_{\gamma_i}^{T(s)}\right|$, normalized to the optimum value above. We call this function the *relative* sensitivity and write it as

$$S_{\gamma_i}(\omega) = \left|\frac{f_i(j\omega)g_i(j\omega)}{T(j\omega)}\right| \tag{4-2}$$

Then if an FSLB filter existed, it would have $S_{\gamma_i}(\omega)=\frac{1}{N}$ for *all* i,ω. The relative sensitivity measure in (4-2) then allows one to see how close a design is to being optimum.

The above measure would still require N plots for integrator sensitivity (one for each integrator). We then define another quantity to be the maximum

relative sensitivity of all integrators,

$$S_{\gamma_i,\infty}(\omega) \triangleq \max_i S_{\gamma_i}(\omega) \tag{4-3}$$

This will be the measure that we will plot to compare the sensitivity of one filter with another.

4.2 Cutsets and Tiesets

In a non-canonic N'th-order ladder one must choose N independent capacitor voltages and inductor currents. The N states simulated must all be independent otherwise we could eliminate one integrator by creating it's output as the sum of others. This would produce a system containing only N-1 integrators, which we know cannot implement a system of order N. It therefore follows that all the capacitive or inductive elements in a tieset or cutset (Fig. 4.1) cannot be simulated as their element voltage or current functions are not all independent.

In a tieset, as in figure 4.1(a),

$$V_{C_1}+V_{C_2}-V_{C_3} = 0 \tag{4-4}$$

so clearly the capacitor voltages V_{C_1}, V_{C_2}, and V_{C_3} are not independent. With a cutset as in the example of figure 4.1(b),

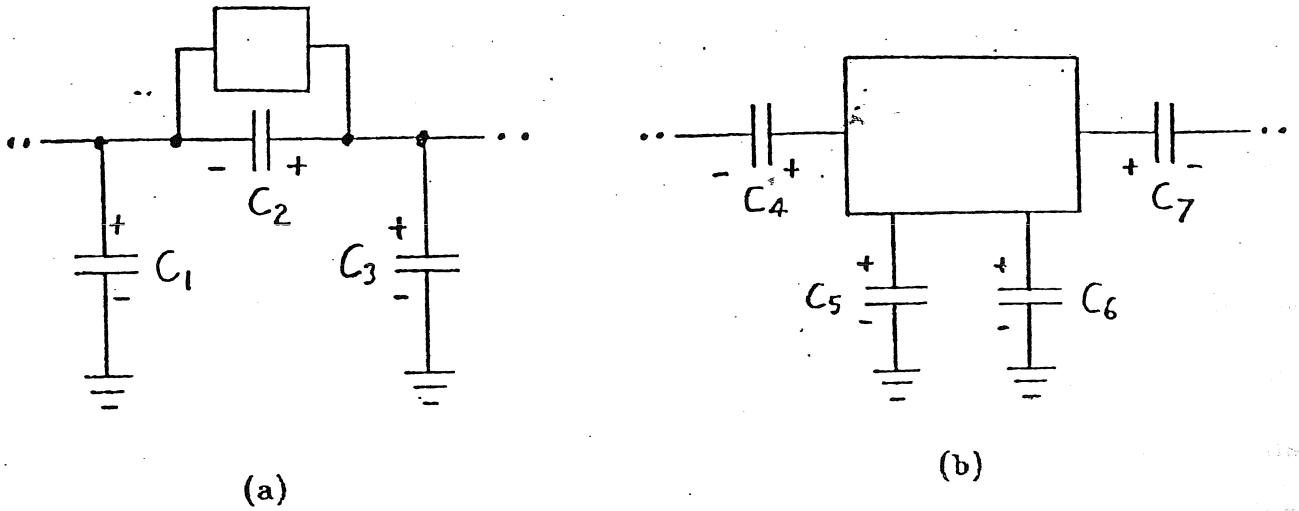

(a) (b)

Figure 4.1 Cutset and tieset examples

$$I_{C_4}+I_{C_5}+I_{C_6}+I_{C_7}=0 \tag{4-5}$$

Integrating equation (4-5) results in

$$C_4V_{C_4}+C_5V_{C_5}+C_6V_{C_6}+C_7V_{C_7}=constant \tag{4-6}$$

which again leads to the capacitor voltages not being independent. Inductive tiesets and cutsets behave in similar manner.

The above constraint of tiesets and cutsets must be satisfied or the canonic realization of the filter is not possible. The eighth order LC ladder described in chapter 3 is shown in figure 3.1. In this circuit there is a cutset described by

$$C_2V_{C_2}+C_3V_{C_3}+C_4V_{C_4}+C_6V_{C_6} = constant \tag{4-7}$$

and a tieset described by

$$V_{C_4}+V_{C_5}+V_{C_6}+V_{C_7} = 0 \tag{4-8}$$

Note that, in this case, two capacitor voltages must not be chosen as states although V_{C_4} breaks both the cutset and the tieset. There are two independent equations relating capacitor voltage dependencies. Therefore the two equations can be combined to eliminate V_{C_4} which would leave an equation not involving V_{C_4}. This equation is

$$C_2V_{C_2}+C_3V_{C_3}-C_4V_{C_5}+(C_6-C_4)V_{C_6}-C_4V_{C_7} = constant \tag{4-9}$$

This equation also shows a dependency which has not been broken though V_{C_4} will not be simulated. This implies that for each cutset or tieset, one element must not be simulated even though an element may break more than one cutset or tieset.

4.3 Voltage or Current Cancellations

Once all cutsets and tiesets have been identified then one element in each is not chosen as a state. There are usually still choices as to which elements in each cutset and tieset should not be used in the simulation. Although the transfer function is obtained with any choice of N independent states, some choices of states cause worse sensitivity than others. As an example, consider

the third order low-pass elliptic filter in figure 3.3.

It is shown in figure 4.2, using computer simulations, that the sensitivity of the resulting active state-space filters are good if V_{C_1}, V_{C_3}, I_{L_2} or V_{C_2}, V_{C_3}, I_{L_2} are chosen as states. The sensitivity becomes poor in the stopband (figure 4.2), if V_{C_1}, V_{C_2}, and I_{L_2} are chosen as states. The reason for poor sensitivity in the last choice is that the output, V_o, is formed as the sum of V_{C_1} and V_{C_2}. At the loss pole $\frac{1}{\sqrt{C_2 L_2}}$, V_o goes to zero which means that V_{C_1} and V_{C_2} must cancel to form zero. Such a method for forming a zero is known to have poor sensitivity. Poor sensitivity is also observed in higher order ladder filters, where the circuit of figure 3.3 is contained in the ladder and V_{C_3} is not chosen as a state. As an example, consider the ladder of figure 3.14. The sensitivity plot for a rather poor realization of this filter is shown in figure 4.3. This realization was obtained by choosing not to simulate V_{C_4}. Note that although V_{C_4} was not chosen as a state, it is still required in the internal workings of the rest of the ladder. The sensitivity plot for a good realization of this same filter is shown in figure 4.4 where the states were chosen according to a rule-of-thumb explained in a later section of this chapter. This leads to the conclusion that element voltages or currents, which go to zero at a loss pole and are formed by a summation of other voltages or currents, should be chosen as states.

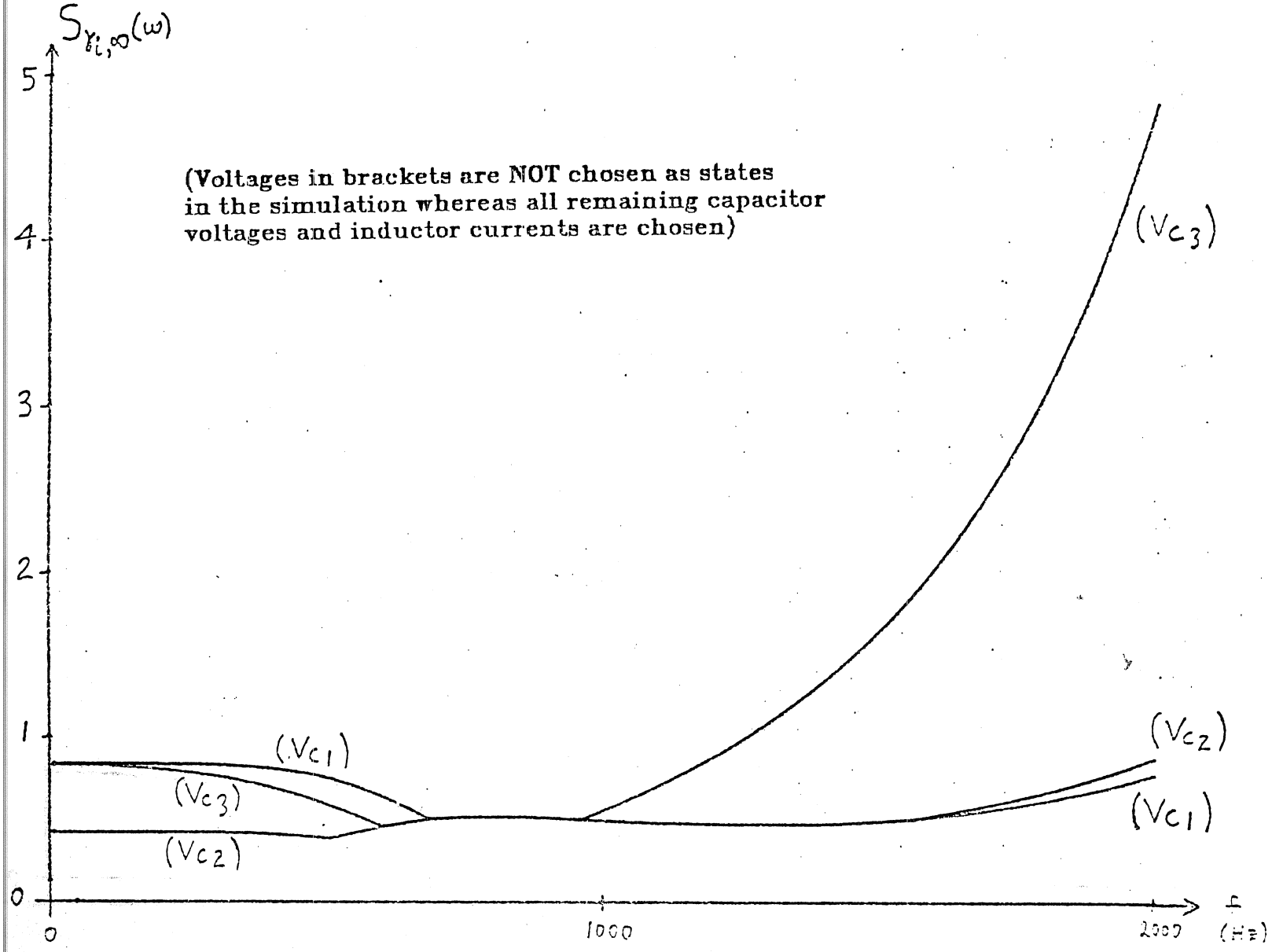

Figure 4.2 Sensitivity for three realizations of third order filter (fig. 3.3) resulting from different choices of states.

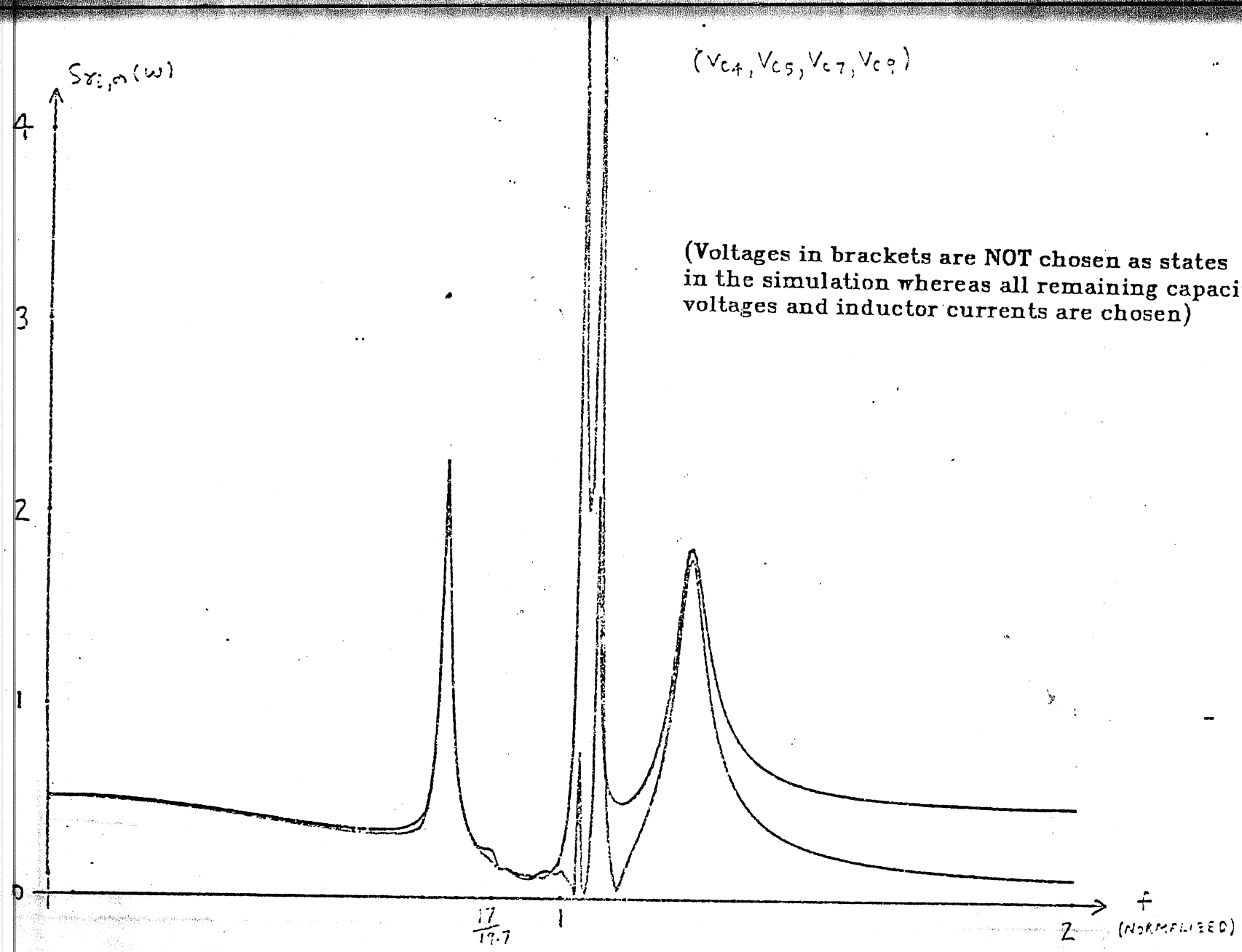

Figure 4.3 Sensitivity for poor realization of twelfth order filter (fig. 3.14).

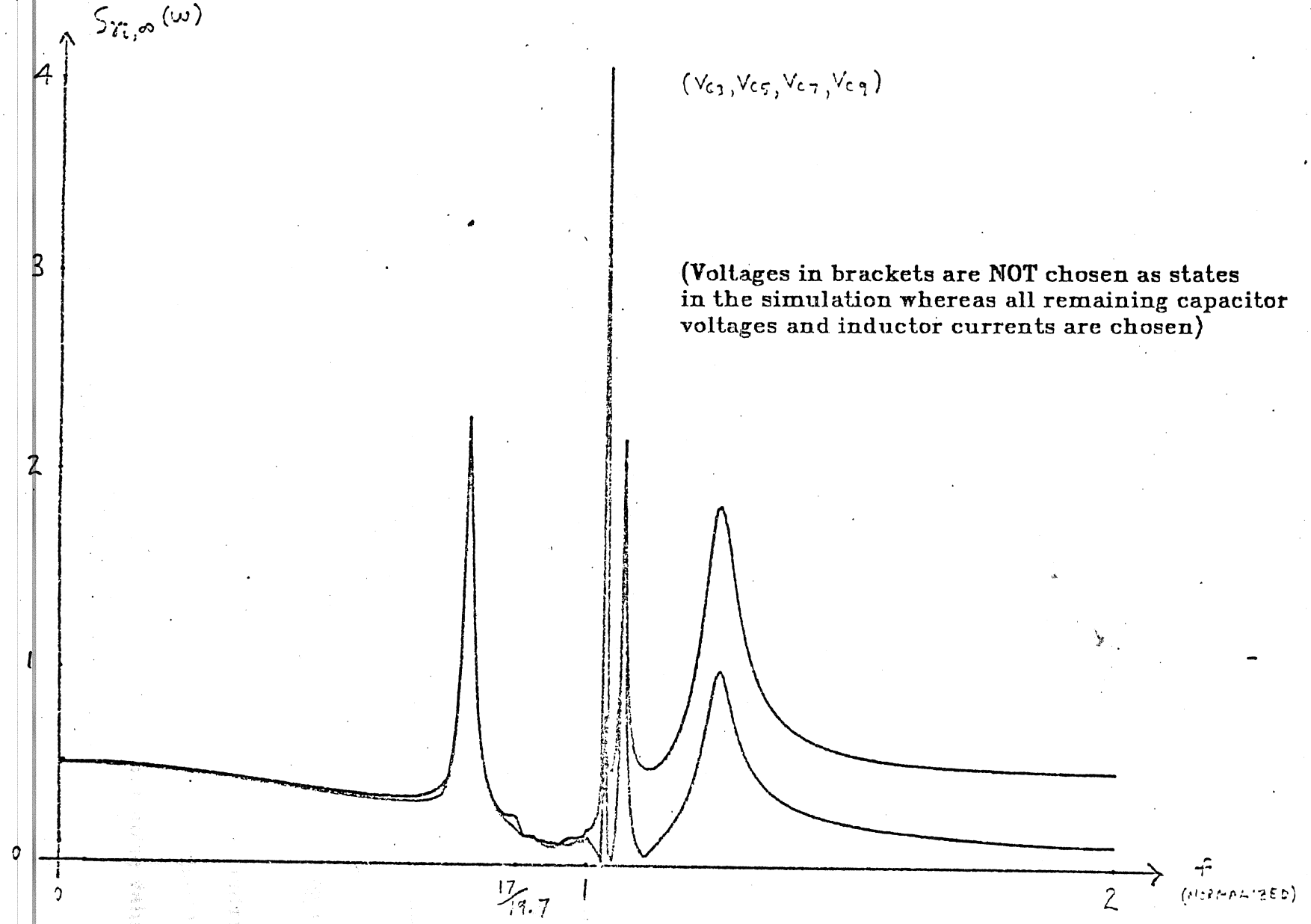

Figure 4.4 Sensitivity for good realization of twelfth order filter (fig. 3.14).

4.4 Closely Correlated States

It was shown that all states of an N'th order state-space system must be independent to create an N'th order transfer function. The question then arises as to what if some of the states are "nearly" dependent: how would one expect the system to perform? In general, the "near" dependent state-space system has poor sensitivity and dynamic range properties. To show that this is the case, we must first define what is meant by "near" dependence.

We define the correlation between two functions f_i and f_j as

$$COR_{ij} \triangleq \frac{\int_{-\infty}^{\infty} \overline{f_i}(j\omega) f_j(j\omega) d\omega}{\|f_i\|_2 \|f_j\|_2} \tag{4-10}$$

If COR_{ij} is 0, then the two functions are orthogonal (in a vector sense), while if COR_{ij} is 1, then the two functions are linearly dependent. "Near" dependence of two functions is then equivalent to their correlation being close to one.

Now if we recall the relationship between **F** and **G** in equation (2-17), namely

$$\mathbf{G}^T = \mathbf{H}\mathbf{F}^{-1} \tag{2-16}$$

we see that if **F** is an ill-conditioned matrix then **G** will contain large entries which in turn means that $\{g_i(s)\}$ will grow. If the set $\{g_i(s)\}$ is large then the resulting state-space system will have poor sensitivity and output noise values as can be seen from the equations of chapter 2.

Since "near" dependent f_i's imply that **F** is ill-conditioned then closely correlated functions chosen as states will produce a system with poor sensitivity and dynamic range results. Therefore, in a ladder, one should not choose pairs of functions which are closely correlated as states. Two cases of capacitor voltage functions which one should avoid choosing together are illustrated in fig. 4.5. It can easily be shown that for fig 4.5(a):

$$V_{C_2} = (1+s^2 L_1 C_1) V_{C_1} \qquad (4\text{-}11)$$

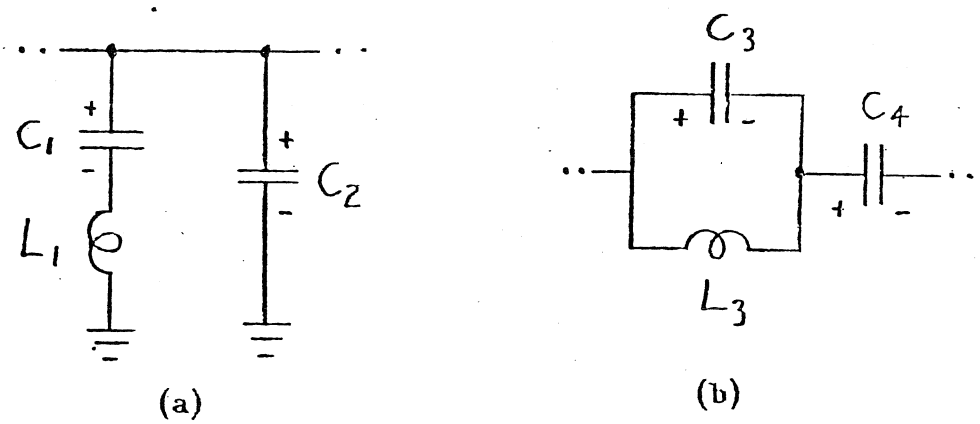

Figure 4.5 Circuits illustrating closely correlated states

Now, we would like to find the approximate correlation between a typical V_{C_1} function and V_{C_2}. If one makes the reasonable assumption that the loss pole $\frac{1}{\sqrt{C_1 L_1}}$ is not in the passband of the filter and that the function V_{C_1} has most of its spectrum on only one side of the loss pole (usually the passband side) then

one can either say

Case 1: passband $< \frac{1}{\sqrt{C_1 L_1}}$

$$V_{C_2} \approx V_{C_1} \quad \omega_1 < \omega < \omega_2 \tag{4-12}$$

or

Case 2: passband $> \frac{1}{\sqrt{C_1 L_1}}$

$$V_{C_2} \approx s^2 L_1 C_1 V_{C_1} \quad \omega_1 < \omega < \omega_2 \tag{4-13}$$

where ω_1, ω_2 define the frequency band which contains the majority of the area under the spectral density curve. This allows us to write

$$\int_{-\infty}^{\infty} |V_{C_1}|(j\omega)d\omega \approx 2\int_{\omega_1}^{\omega_2} |V_{C_1}|(j\omega)d\omega \tag{4-14}$$

since $|V_{C_1}|$ is near zero outside these bounds.

From (4-10), we can write

$$corr = \frac{\int_{-\infty}^{\infty} \overline{V_{C_1}}(j\omega)V_{C_2}(j\omega)d\omega}{\|V_{C_1}\|_2 \|V_{C_2}\|_2} \tag{4-15}$$

And so for case 1, since $V_{C_2} = V_{C_1}$ for all ω between ω_1, ω_2 then

$$corr_1 \approx \frac{\int_{-\infty}^{\infty} \overline{V_{C_1}}(j\omega) V_{C_1}(j\omega) d\omega}{\|V_{C_1}\|_2 \|V_{C_1}\|_2} = 1 \qquad (4\text{-}16)$$

We know from before that if two functions are closely correlated (as V_{C_1} and V_{C_2} are in this case) then they should not both be chosen as states. Also in case 2, since $V_{C_2} = s^2 L_1 C_1 V_{C_1}$ for all ω between ω_1, ω_2 then

$$corr_2 \approx \frac{L_1 C_1 \int_{-\infty}^{\infty} \overline{V_{C_1}}(j\omega)(-\omega^2) V_{C_1}(j\omega) d\omega}{\|V_{C_1}\|_2 L_1 C_1 \|(-\omega^2) V_{C_1}\|_2} \qquad (4\text{-}17)$$

and if we also say that ω does not change much over $\omega_1 < \omega < \omega_2$ then

$$corr_2 \approx \frac{L_1 C_1 \|V_{C_1}\|_2^2}{\|V_{C_1}\|_2 L_1 C_1 \|V_{C_1}\|_2} = 1 \qquad (4\text{-}18)$$

Again we have that the correlation between V_{C_1} and V_{C_2} is close to one so they should not both be chosen as states.

In figure 4.5(b) the relation between the capacitor voltages is

$$V_{C_4} = \left[\frac{1+s^2 L_3 C_3}{s^2 L_3 C_4}\right] V_{C_3} \qquad (4\text{-}19)$$

Here again, either the s^2 terms will cancel and the two functions will be close to being dependent or the functions will be related by an s^2 term. Of course, if we draw the dual of the circuits in figure 4.5, there will be two similar situations where two pairs of inductor currents will be nearly dependent. And as

explained before, we should not choose pairs of functions which are closely correlated to be states. As an example of the application of this rule, consider the eighth order filter of figure 3.1. If one chooses as states both V_{C_5} and V_{C_6}, then the resulting filter has both poor sensitivity and output noise figures. Figure 4.6 shows the sensitivity plot while figure 4.7 shows the output noise plot of this simulation which chooses "near" dependent states. Also shown on the same plots are curves of sensitivity and output noise from a good simulation of this same ladder.

4.5 Breaking a cutset and tieset twice

Another choice of states leading to poor sensitivity is choosing not to simulate V_{C_4} and V_{C_6} in the filter of figure 3.1. The reason for this is that by leaving out these two states the cutset and tieset are both broken *twice*. This causes more difficulties for the simulation as it must in effect solve a simultaneous set of equations to obtain V_{C_4} or V_{C_6} (rather than doing so through a simple summation). Figure 4.8 shows the sensitivity plot for the realization in which V_{C_4} and V_{C_6} are both not chosen as states. On the same plot are two sensitivity curves for good simulations of this same filter. One good simulation is where V_{C_4} and V_{C_5} are not chosen as states while the other is the simulation where V_{C_3} and V_{C_6} are not chosen as states.

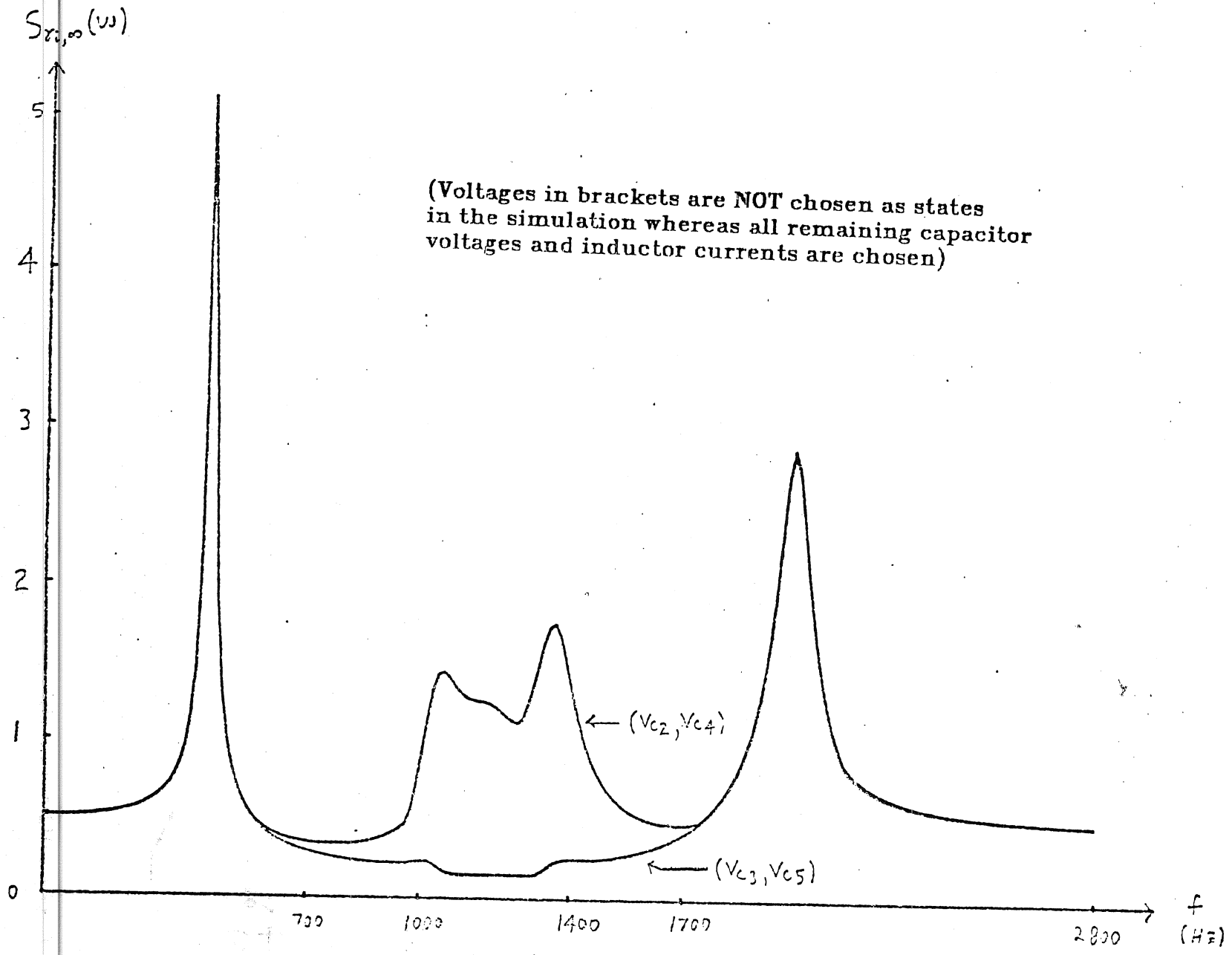

Figure 4.6 Sensitivity for two realizations of eighth order filter (fig. 3.1). (V_{C_2}, V_{C_4}) simulates two closely correlated states.

(Voltages in brackets are NOT chosen as states in the simulation whereas all remaining capacitor voltages and inductor currents are chosen)

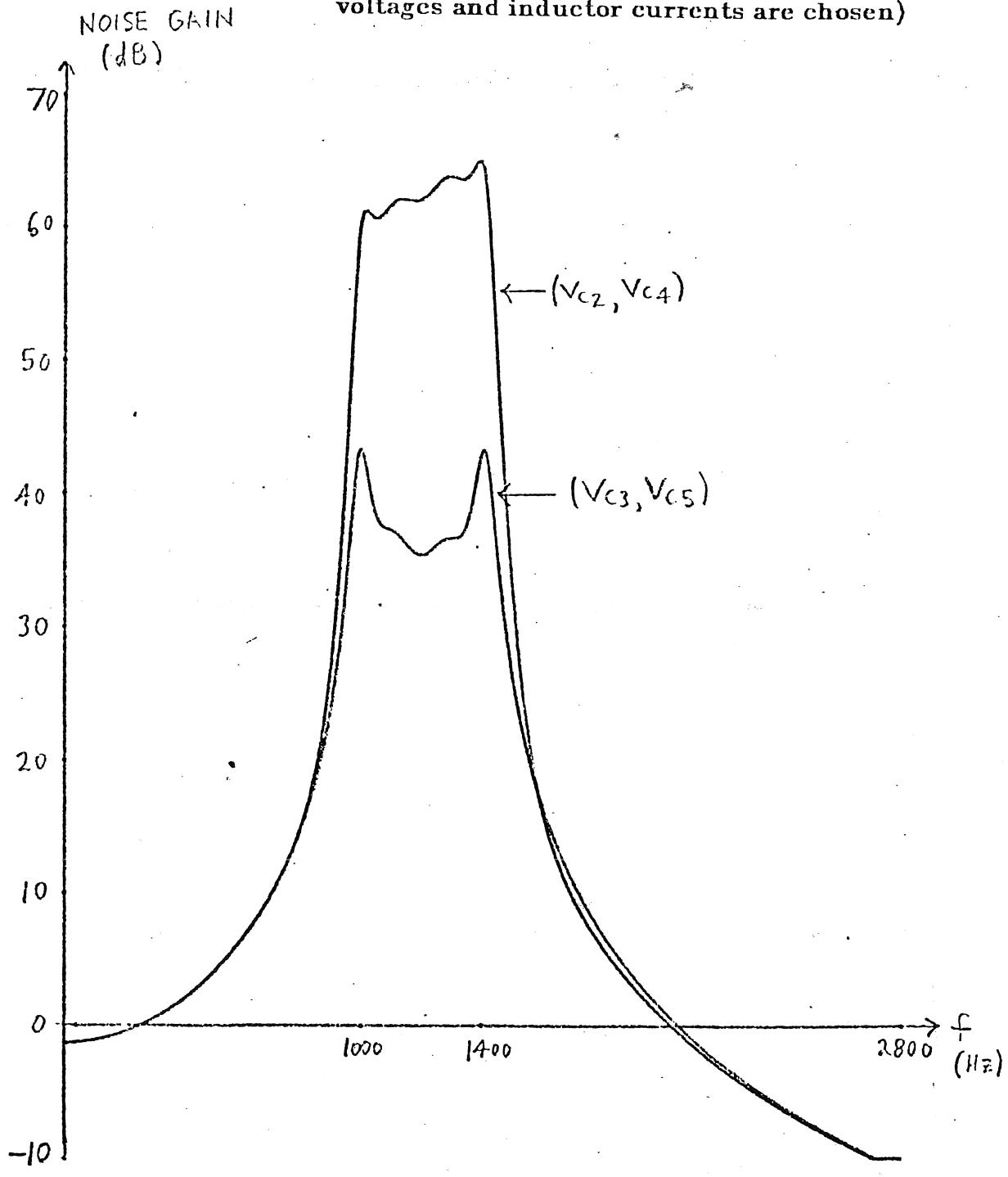

Figure 4.7 Output noise for two realizations of eighth order filter (fig. 3.1)

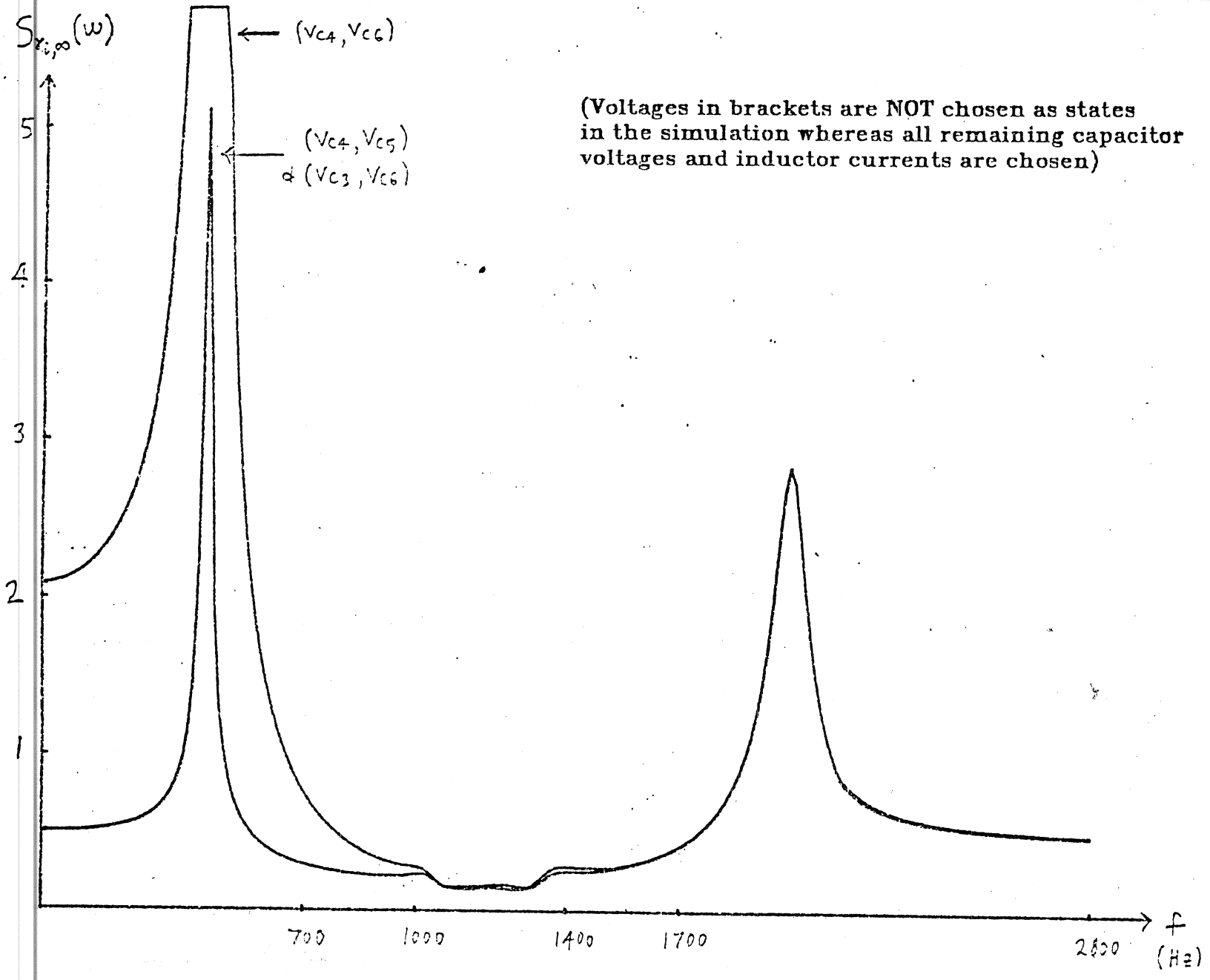

(Voltages in brackets are NOT chosen as states in the simulation whereas all remaining capacitor voltages and inductor currents are chosen)

Figure 4.8 Sensitivity for three realizations of eighth order filter (fig. 3.1). (V_{C_4}, V_{C_5}) breaks cutset and tieset twice.

4.6 A Rule of Thumb

All of the rules above may be satisfied by only breaking the cutsets and tiesets of a ladder using elements in a resonant tank which forms a loss pole. In the above eighth order LC ladder V_{C_3} and V_{C_5} are the element voltages which should not be simulated. There might be a choice as to which element in the tanks to choose as in fig. 4.9 below. Using computer simulations, as shown in figure 4.10, it was found that the sensitivity results are the same for both choices. One can either choose V_{C_3} and I_{L_4} or I_{L_3} and V_{C_4} but only one element voltage or current in each tank is not simulated as a state, and both tiesets must be broken.

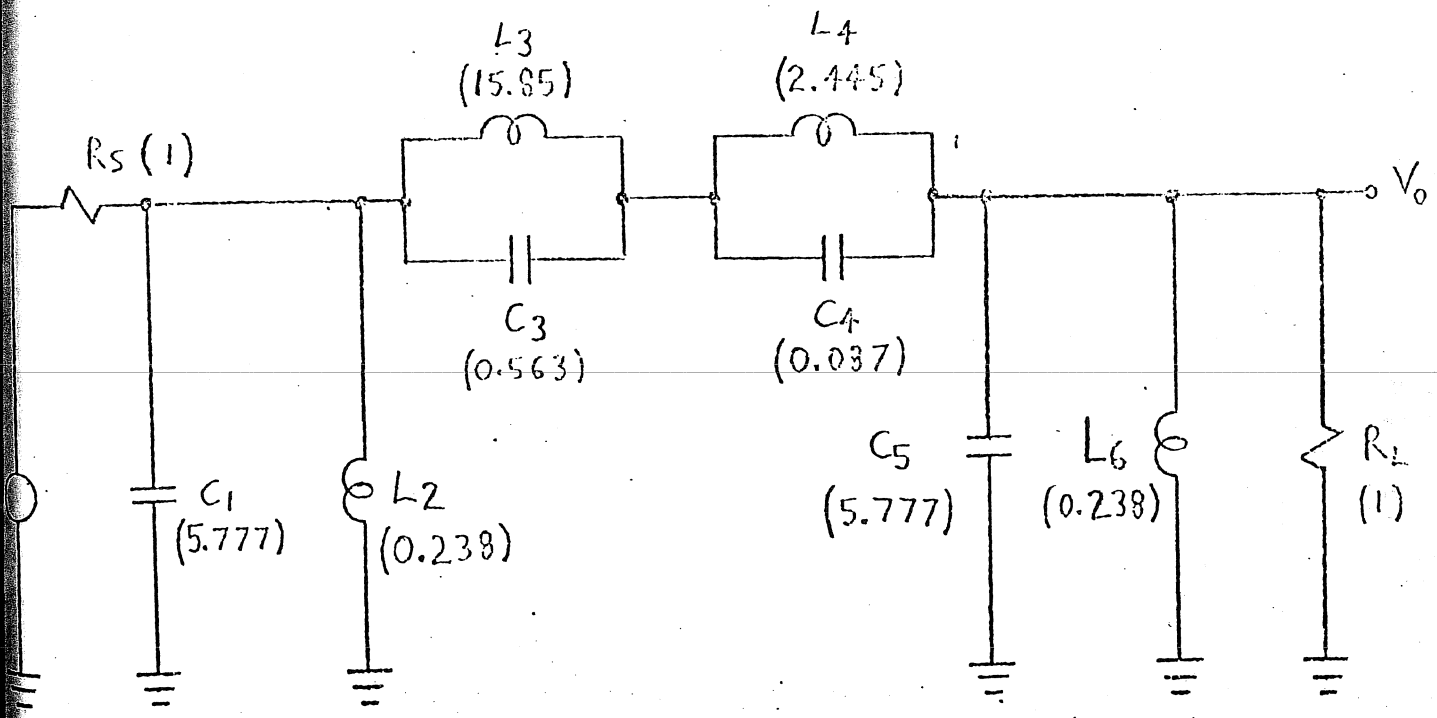

Figure 4.9 Sixth order LC ladder

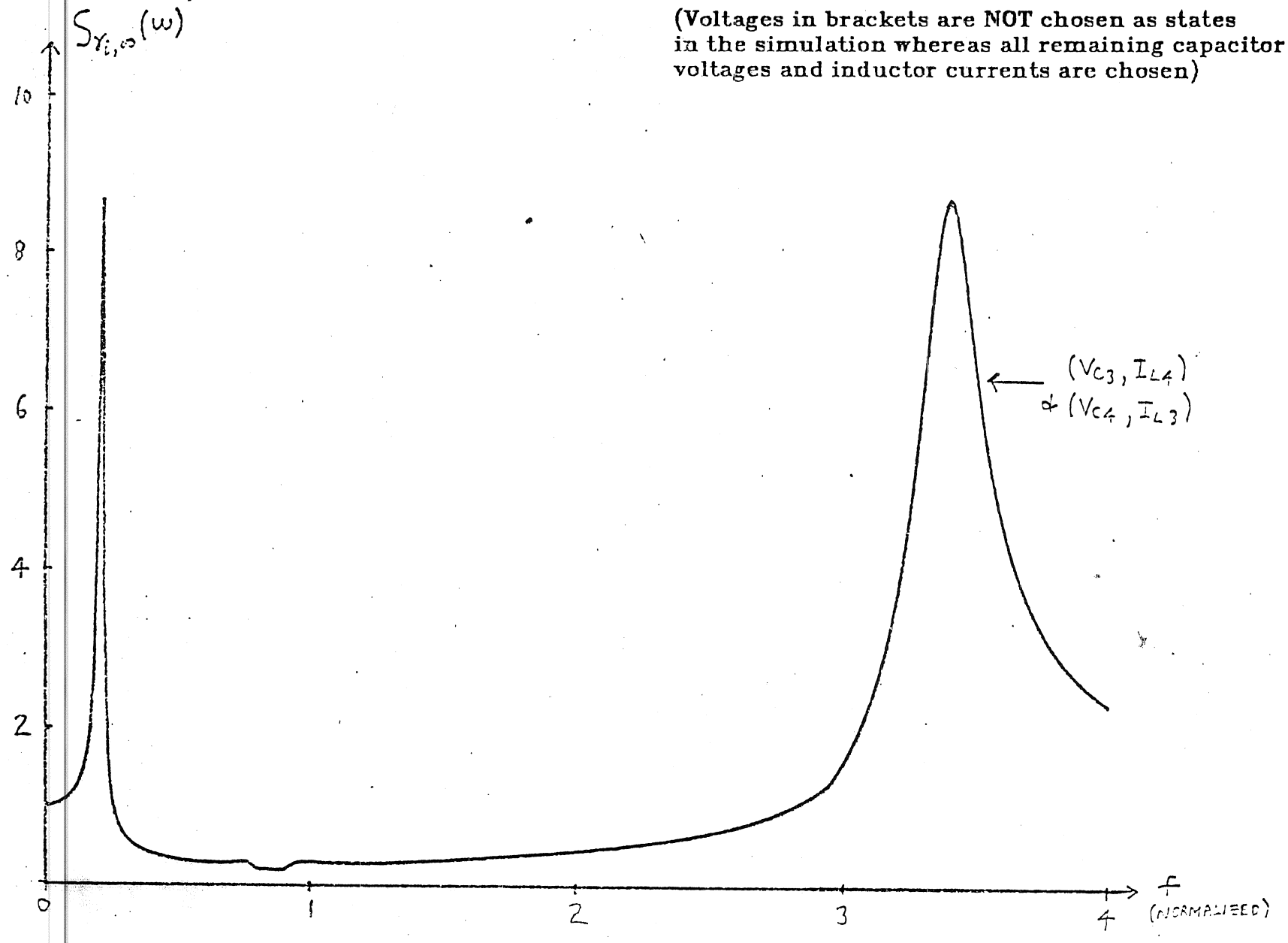

Figure 4.10 Sensitivity for two realizations of sixth order filter (fig. 4.9). Note that the sensitivities are the same for two choices which follow rule-of-thumb.

4.7 Conclusions

Ladders typically present good choices for states of a state-space system that realize a given N'th order transfer function. With the simulation of a canonic LC ladder, the sensitivity figures of the integrator-gain of each integrator in a state-space simulation is directly related to the sensitivity figures of the passive elements in the LC ladder. Because of this, a state-space active simulation of a canonic ladder will have the same good sensitivity properties as the LC ladder.

In the case of a non-canonic LC ladder, one must be careful to choose a set of states from the ladder that does not adversely affect the sensitivity of the system. If the choice is done properly the resulting simulation will also have the low sensitivity properties of the LC ladder. We have attempted to provide some insight as to why choosing certain sets of states from a non-canonic ladder can create a system with poor sensitivity performance. Together with this insight, some rules have been given so that one may avoid choosing a bad set of states. Finally, a rule-of-thumb was presented which, when followed, helps one to choose a good set of states which then can be used to synthesize a state-space filter as will be shown in the next chapter.

5. Design Procedure

This chapter will present the design details of how one obtains a scaled state-space system from an N'th order doubly terminated LC ladder. An active RC circuit can then be easily obtained from the scaled system as shown in chapter 2.

An interesting feature of this design method is that most state-space systems can be easily found by algebraic manipulations as will be demonstrated by some examples. For larger systems, a procedure well suited to computers is presented.

5.1 Obtaining State Equations from a Ladder

The first step after obtaining an N'th order LC ladder to simulate is to choose N capacitor voltages and inductor currents which will be states in the state-space system. This choice should be made according to the rules of chapter 4. Note that for a canonic ladder, there is only one choice which is to use all inductor currents and capacitor voltages as states.

The state equations are then obtained by writing equations about each element whose voltage or current is to be simulated. For each capacitor whose voltage has been chosen as a state to be simulated, we write a node equation expressing the current through the capacitor in terms of the other state

variables. Similarly, for each inductor whose current has been chosen as a state, we write a loop equation expressing the voltage across the inductor in terms of the other state variables. All equations should only contain element voltages or currents which are states. This is possible through the use of the cutset and tieset dependencies. All "s" terms are then gathered on the left side of each equation leaving only the input and chosen states (not multiplied by "s") on the right hand side of the equation. These equations can be put in the following form

$$\mathbf{M}s\mathbf{x} = \mathbf{N}\mathbf{x}+\mathbf{R}V_i \tag{5-1}$$

where $\mathbf{x}$ is, as before, an N x 1 vector of states; V_i is the input voltage; $\mathbf{M}$ and $\mathbf{N}$ are N x N real matrices; and $\mathbf{R}$ is an N x 1 real matrix. We wish to solve for the derivative of the states so that the above equation is in the form:

$$s\mathbf{x} = \mathbf{A}\mathbf{x}+\mathbf{b}u \tag{5-2}$$

This can be done by multiplying both sides of (5-1) by $\mathbf{M}^{-1}$ to obtain

$$s\mathbf{x} = \mathbf{M}^{-1}\mathbf{N}\mathbf{x}+\mathbf{M}^{-1}\mathbf{R}V_i \tag{5-3}$$

$$\triangleq \mathbf{A}\mathbf{x}+\mathbf{b}u \tag{5-4}$$

so we see that

$$\mathbf{A} = \mathbf{M}^{-1}\mathbf{N} \tag{5-5}$$

$$\mathbf{b} = \mathbf{M}^{-1}\mathbf{R} \tag{5-6}$$

For most LC ladder simulations, one will find that **M** is close to being a diagonal matrix. If this is the case, then keeping the left and right hand sides of (5-1) separated, one can solve for the derivatives of the states using simple algebraic manipulations. This method will become more obvious once demonstrated.

To obtain the **c** vector and d scalar of the state-space system, we first look at the four possible termination configurations of an LC doubly terminated ladder shown in figure 5.1. The N'th inductor current or capacitor voltage should be chosen as a state since without it a final summation is required to obtain the desired transfer function of the circuit.

In figure 5.1(a), V_{C_N} is the output of the N'th integrator so

$$V_o = V_{C_N} \tag{5-7}$$

from which $\mathbf{c}^T$ and d can be seen to be

$$\mathbf{c}^T = [0\ 0\ \cdots\ 1] \quad d = 0 \tag{5-8}$$

In figure 5.1(b), I_{L_N} is the output of the N'th integrator so

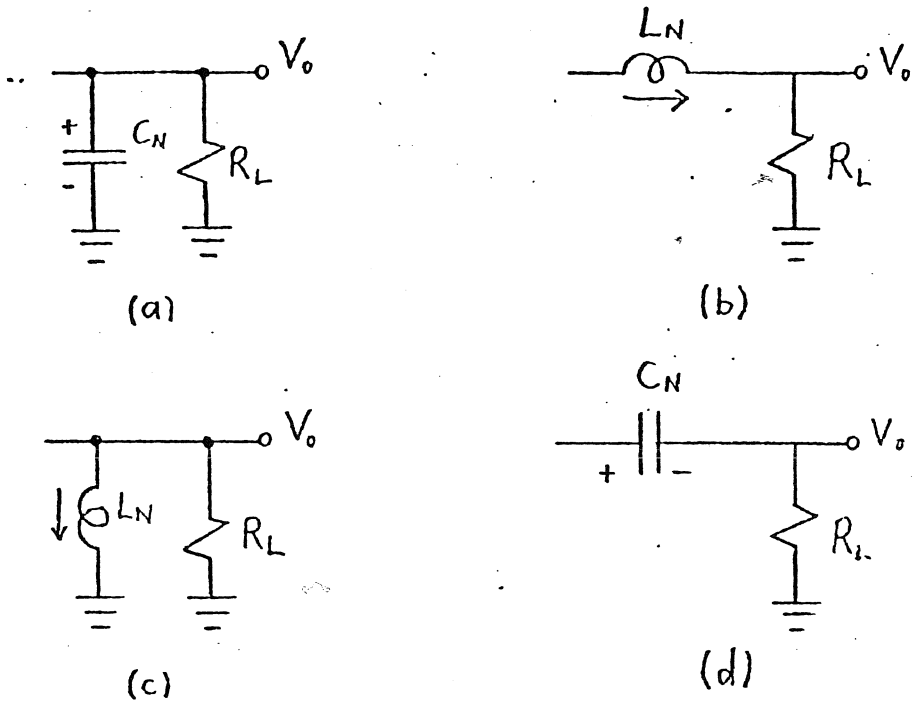

Figure 5.1 Doubly terminated ladder termination configurations

$$V_o = I_{L_N} R_L \tag{5-9}$$

from which $\mathbf{c}^T$ and d are seen to be

$$\mathbf{c}^T = [0\ 0\ \cdots\ R_L] \quad d = 0 \tag{5-10}$$

As the next two cases are more complicated, it is advantagous for the designer to try to find an LC ladder which has terminations as in 5.1 (a) or (b). If this is not possible, then we continue with (c) and (d).

In figure 5.1(c), I_{L_N} is the output while $sL_N I_{L_N}$ is the input of the N'th integrator, so

$$V_o = sL_N I_{L_N} \tag{5-11}$$

and therefore $\mathbf{c}^T$ is proportional to the N'th row of **A** while d is proportional to the N'th element of **b**, ie.

$$\mathbf{c}^T = \begin{bmatrix} L_N A_{N1} & L_N A_{N2} & \cdots & L_N A_{NN} \end{bmatrix} \quad d = L_N b_N \tag{5-12}$$

In figure 5.1(d), V_{C_N} is the output and and $sC_N V_{C_N}$ is the input of the N'th integrator, so

$$V_o = sC_N V_{C_N} R_L \tag{5-13}$$

and therefore $\mathbf{c}^T$ is proportional to the N'th row of **A** while d is proportional to the N'th element of **b**, ie.

$$\mathbf{c}^T = \begin{bmatrix} C_N R_L A_{N1} & C_N R_L A_{N2} & \cdots & C_N R_L A_{NN} \end{bmatrix} \quad d = C_N R_L b_N \tag{5-14}$$

Using the above method to find **c** and d causes the transfer function, $\frac{y}{u}$, to have the same gain as the LC ladder transfer function, $\frac{V_o}{V_i}$. This gain can be scaled to the required filter gain before scaling the rest of the filter for optimum dynamic range. If the required filter gain relative to the LC ladder gain is k then one scales the gain of $\frac{y}{u}$ by multiplying $\mathbf{c}^T$ and d by k. This will be seen in the examples that follow.

5.2 Design Examples

5.2.1 Fifth Order Canonic Example

Consider the fifth order Chebyshev low-pass filter shown in figure 5.2 below and assume that we wish to design an active simulation of this filter with a DC gain of unity.

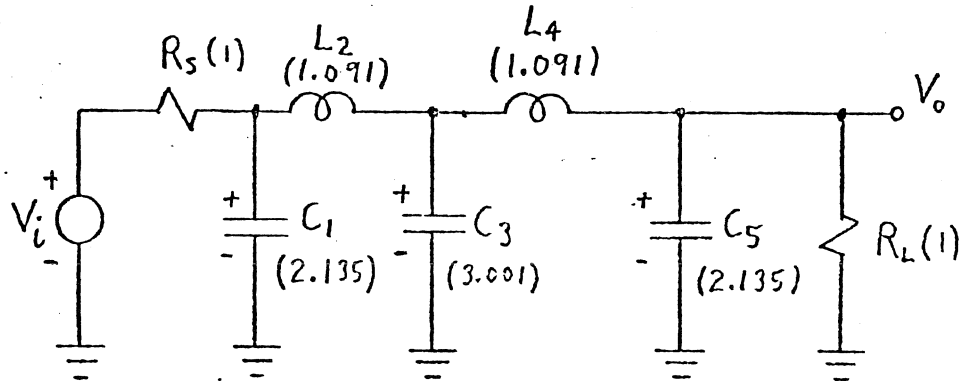

Figure 5.2 Fifth order canonic ladder

Since this is a canonic ladder, all the inductor currents and capacitor voltages are chosen as states.

Writing the node equations for C_1, C_3, and C_5, as explained above, gives

$$sC_1V_{C_1} = \frac{V_i - V_{C_1}}{R_s} - I_{L_2} \tag{5-15}$$

$$sC_3V_{C_3} = I_{L_2} - I_{L_4} \tag{5-16}$$

$$sC_5V_{C_5} = I_{L_4} - \frac{V_{C_5}}{R_L} \tag{5-17}$$

Writing the loop equations for L_2 and L_4 gives

$$sL_2I_{L_2} = V_{C_1} - V_{C_3} \tag{5-18}$$

$$sL_4I_{L_4} = V_{C_3} - V_{C_5} \tag{5-19}$$

Arranging these equations in order (for illustrative purposes only) and substituting in the element values, we obtain

$$2.135sV_{C_1} = -V_{C_1} - I_{L_2} + V_i \tag{5-20}$$

$$1.091sI_{L_2} = V_{C_1} - V_{C_3} \tag{5-21}$$

$$3.001sV_{C_3} = I_{L_2} - I_{L_4} \tag{5-22}$$

$$1.091sI_{L_4} = V_{C_3} - V_{C_5} \tag{5-23}$$

$$2.135sV_{C_5} = I_{L_4} - V_{C_5} \tag{5-24}$$

So, in the form of (5-1), these equations may be written as

$$\begin{bmatrix} 2.135 & 0 & 0 & 0 & 0 \\ 0 & 1.091 & 0 & 0 & 0 \\ 0 & 0 & 3.001 & 0 & 0 \\ 0 & 0 & 0 & 1.091 & 0 \\ 0 & 0 & 0 & 0 & 2.135 \end{bmatrix} \begin{bmatrix} sV_{C_1} \\ sI_{L_2} \\ sV_{C_3} \\ I_{L_4} \\ V_{C_5} \end{bmatrix} = \tag{5-25}$$

$$\begin{bmatrix} -1 & -1 & 0 & 0 & 0 \\ 1 & 0 & -1 & 0 & 0 \\ 0 & 1 & 0 & -1 & 0 \\ 0 & 0 & 1 & 0 & -1 \\ 0 & 0 & 0 & 1 & -1 \end{bmatrix} \begin{bmatrix} V_{C_1} \\ I_{L_2} \\ V_{C_3} \\ I_{L_4} \\ V_{C_5} \end{bmatrix} + \begin{bmatrix} 1 \\ 0 \\ 0 \\ 0 \\ 0 \end{bmatrix} V_i$$

Then $\mathbf{M}^{-1}$ is

$$\mathbf{M}^{-1} = \begin{bmatrix} 0.468 & 0 & 0 & 0 & 0 \\ 0 & 0.917 & 0 & 0 & 0 \\ 0 & 0 & 0.333 & 0 & 0 \\ 0 & 0 & 0 & 0.917 & 0 \\ 0 & 0 & 0 & 0 & 0.468 \end{bmatrix} \tag{5-26}$$

If we use (5-5) and (5-6), then the state-space matrices are

$$\mathbf{A} = \begin{bmatrix} -0.468 & -0.468 & 0 & 0 & 0 \\ 0.917 & 0 & -0.917 & 0 & 0 \\ 0 & 0.333 & 0 & -0.333 & 0 \\ 0 & 0 & 0.917 & 0 & -0.917 \\ 0 & 0 & 0 & 0.468 & -0.468 \end{bmatrix} \quad \mathbf{b} = \begin{bmatrix} 0.468 \\ 0 \\ 0 \\ 0 \\ 0 \end{bmatrix} \tag{5-27}$$

From figure 5.1 and the ladder, we see that

$$V_o = V_{C_5} \tag{5-28}$$

so $\mathbf{c}$ and d are simply

$$\mathbf{c}^T = \begin{bmatrix} 0 & 0 & 0 & 0 & 1 \end{bmatrix} \quad d = 0 \tag{5-29}$$

Also, it can be easily shown that the DC gain of the ladder is .5 so we should scale $\mathbf{c}^T$ by our desired DC gain (1) divided by the DC gain of the ladder (.5).

Then $\mathbf{c}^T$ becomes

$$\mathbf{c}^T = \begin{bmatrix} 0 & 0 & 0 & 0 & 2 \end{bmatrix} \quad d = 0 \tag{5-30}$$

Obtaining $\mathbf{A}$ and $\mathbf{b}$ as shown above may be called a matrix method of solution.

An algebraic method to obtain these matrices for this example would proceed as follows. We isolate the derivatives of the states of equations (5-20)-(5-24) so the equations appear as

$$sV_{C_1} = -0.469V_{C_1} - 0.468I_{L_2} + 0.468V_i \tag{5-31}$$

$$sI_{L_2} = 0.917V_{C_1} - 0.917V_{C_3} \tag{5-32}$$

$$sV_{C_3} = 0.333I_{L_2} - 0.333I_{L_4} \tag{5-33}$$

$$sI_{L_4} = 0.917V_{C_3} - 0.917V_{C_5} \tag{5-34}$$

$$sV_{C_5} = 0.468I_{L_4} - 0.468V_{C_5} \tag{5-35}$$

From these equations, **A** and **b** can be directly written and are, of course, the same as those obtained using the matrix method.

5.2.2 Third Order Non-Canonic Example

As an example of a non-canonic ladder, consider the third order low-pass ladder filter in fig. 3.3 shown again in figure 5.3. It is normalized so that its upper passband edge is at 1 rad/sec and its stopband begins at 1.4 rad/sec. The passband has a ripple of 1 dB and the stopband minimum attenuation is 22 dB. From these specifications this ladder can be designed using a filter design program or filter tables. We will design a state-space system where the DC gain is 1.

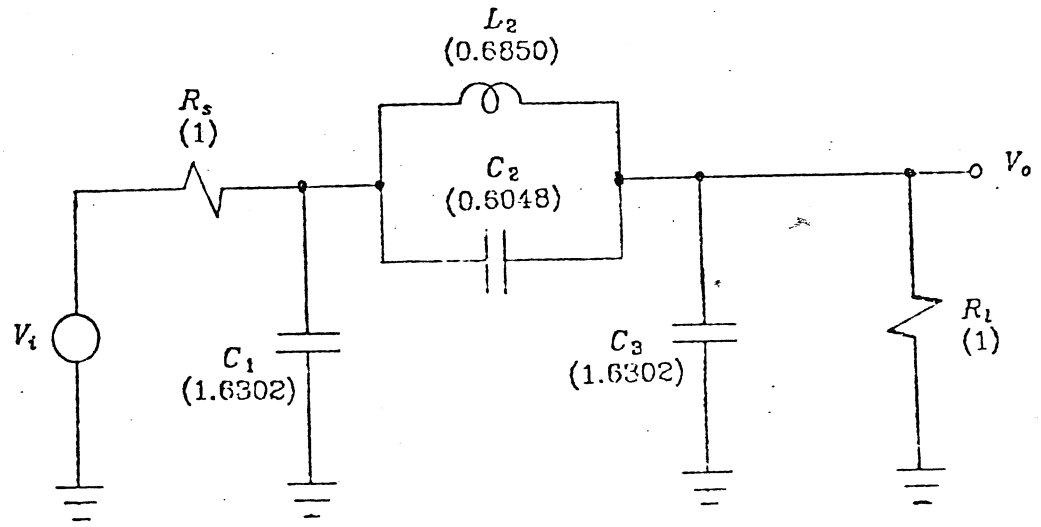

Figure 5.3 Third order lowpass ladder (same as in figure 3.3)

Only three states will be simulated since it is a third order filter. These states are chosen to be V_{C_1}, I_{L_2}, and V_{C_3}. The capacitor voltage in the resonant tank is not simulated. The state equations are found by first writing 3 independent equations involving the capacitor voltages and inductor currents chosen as states. These equations are:

$$sC_1V_{C_1} = \frac{1}{R_s}(V_i - V_{C_1}) + sC_2(V_{C_3} - V_{C_1}) - I_{L_2} \tag{5-36}$$

$$sL_2I_{L_2} = V_{C_1} - V_{C_3} \tag{5-37}$$

$$sC_3V_{C_3} = \frac{-1}{R_l}(V_{C_3})+sC_2(V_{C_1}-V_{C_3})+I_{L_2} \tag{5-38}$$

Next, all s terms are gathered on the left side of each equation to give:

$$sV_{C_1}(C_1+C_2)-sV_{C_3}(C_2) = \frac{1}{R_s}(V_i-V_{C_1})-I_{L_2} \tag{5-39}$$

$$sI_{L_2}(L_2) = V_{C_1}-V_{C_3} \tag{5-40}$$

$$-sV_{C_1}(C_2)+sV_{C_3}(C_2+C_3) = \frac{-1}{R_l}(V_{C_3})+I_{L_2} \tag{5-41}$$

Proceeding with the algebraic method to obtain **A** and **b**, we solve for sV_{C_1}, sI_{L_2}, and sV_{C_3} treating the right hand side of each equation as a constant. This gives :

$$sV_{C_1} = V_i\left[\frac{1}{R_s}\left[\frac{C_2+C_3}{(C_1+C_2)(C_2+C_3)-C_2^2}\right]\right]+V_{C_1}\left[\frac{-1}{R_s}\left[\frac{C_2+C_3}{(C_1+C_2)(C_2+C_3)-C_2^2}\right]\right]$$

$$+I_{L_2}\left[\frac{-C_3}{(C_1+C_2)(C_2+C_3)-C_2^2}\right]+V_{C_3}\left[\frac{-1}{R_l}\left[\frac{C_2}{(C_1+C_2)(C_2+C_3)-C_2^2}\right]\right] \tag{5-42}$$

$$sI_{L_2} = V_{C_1}\left[\frac{1}{L_2}\right] - V_{C_3}\left[\frac{1}{L_2}\right] \tag{5-43}$$

$$sV_{C_3} = V_i\left[\frac{1}{R_s}\left[\frac{C_2}{(C_1+C_2)(C_2+C_3)-C_2^2}\right]\right] + V_{C_1}\left[\frac{-1}{R_s}\left[\frac{C_2}{(C_1+C_2)(C_2+C_3)-C_2^2}\right]\right]$$

$$+I_{L_2}\left[\frac{C_1}{(C_1+C_2)(C_2+C_3)-C_2^2}\right] + V_{C_3}\left[\frac{-1}{R_l}\left[\frac{C_1+C_2}{(C_1+C_2)(C_2+C_3)-C_2^2}\right]\right] \tag{5-44}$$

The above are the state-space equations for the LC ladder of figure 5. when V_{C_2} is not simulated. Note that the above equations are fairly large for a general third order low pass filter ladder. With a higher order, it is advantageous to simulate a specific ladder (ie. known element values) and put in the element values when first writing the equations. Substituting in equations (5-42), (5-43), and (5-44) the values for R_s, R_l, C_1, C_2, C_3, and L_2 gives the following equations.

$$sV_{C_1} = 0.4828V_i - 0.4828V_{C_1} - 0.3521I_{L_2} - 0.1306V_{C_3} \tag{5-45}$$

$$sI_{L_2} = 1.460V_{C_1} - 1.460V_{C_3} \tag{5-46}$$

$$sV_{C_3} = 0.1306V_i - 0.1306V_{C_1} + 0.3521I_{L_2} - 0.4828V_{C_3} \tag{5-47}$$

From the above equations the state-space matrices **A**, and **b** can be easily written as

$$\mathbf{A} = \begin{bmatrix} -0.4828 & -0.3521 & -0.1306 \\ 1.460 & 0 & -1.460 \\ -0.1306 & 0.3521 & -0.4828 \end{bmatrix} \qquad \mathbf{b} = \begin{bmatrix} 0.4828 \\ 0 \\ 0.1306 \end{bmatrix} \tag{5-48}$$

Then using the same approach as in the canonic example to find $\mathbf{c}$ and d we find

$$\mathbf{c}^T = \begin{bmatrix} 0 \\ 0 \\ 2 \end{bmatrix} \qquad d = 0 \tag{5-49}$$

If we wish to use the matrix method to find the state-space matrices, then from equations (5-45)-(5-47), we substitute in the element values and write **M**, **N**, and **R**. These are

$$\mathbf{M} = \begin{bmatrix} 2.235 & 0 & -0.6048 \\ 0 & 0.6850 & 0 \\ -0.6048 & 0 & 2.235 \end{bmatrix} \quad \mathbf{N} = \begin{bmatrix} -1 & -1 & 0 \\ 1 & 0 & -1 \\ 0 & 1 & -1 \end{bmatrix} \quad \mathbf{R} = \begin{bmatrix} 1 \\ 0 \\ 0 \end{bmatrix} \tag{5-50}$$

Then one can easily find $\mathbf{M}^{-1}$ to be

$$\mathbf{M}^{-1} = \begin{bmatrix} 0.4828 & 0 & 0.1306 \\ 0 & 1.460 & 0 \\ 0.1306 & 0 & 0.4828 \end{bmatrix} \tag{5-51}$$

Using equations (5-5) and (5-6) one finds the same **A** and **b** matrices as when using the algebraic method.

5.2.3 Eighth Order Bandpass Filter Example

As a third example, recall the eighth order LC ladder of figure 3.1 which is repeated in figure 5.4.

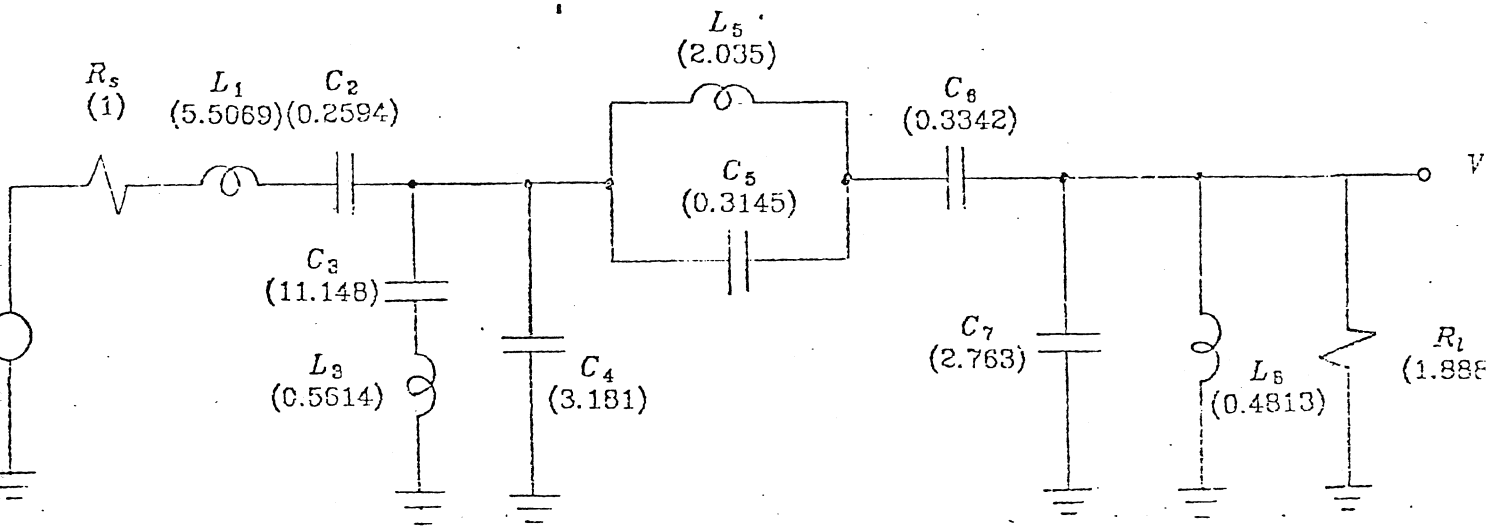

Figure 5.4 Eighth order bandpass ladder (same as in figure 3.1)

We wish to design a state-space system from this ladder where the gain at reflection zeros is one. Choosing to not simulate V_{C_3} and V_{C_5}, eight independent equations may be written involving the eight chosen states. All of these equations are straightforward except for the loop equation involving I_{L_3}. For this third equation, a loop equation is written around the third and fourth arm of the LC ladder. This equation is

$$sL_3I_{L_3}+V_{C_3}-V_{C_4}=0 \tag{5-52}$$

but V_{C_3} was not chosen as a state so it must be eliminated from this equation.

The voltage V_{C_3} was not chosen as a state so as to break up the cutset involving V_{C_2}, V_{C_4}, V_{C_6}, and of course, V_{C_3}. We can then use this cutset's information to find a representation for V_{C_3} which involves only voltages chosen as states. The cutset's dependency is represented by

$$-I_{C_2}+I_{C_3}+I_{C_4}+I_{C_6} = 0 \tag{5-53}$$

which is equivalent to

$$-sC_2V_{C_2}+sC_3V_{C_3}+sC_4V_{C_4}+sC_6V_{C_6} = 0 \tag{5-54}$$

dividing through by "s", we obtain an equation which equals a constant. We lose no information if we force this constant to be zero since the filter we are simulating has at least one loss pole at DC. The equation which relates the voltages involved in the cutset is then

$$V_{C_3} = \frac{C_2}{C_3}V_{C_2}-\frac{C_4}{C_3}V_{C_4}-\frac{C_6}{C_3}V_{C_6} \tag{5-55}$$

Now, substituting the above equation into (5-54), the third state equation is found.

The eight equations are

$$sL_1I_{L_1}+R_sI_{L_1}+V_{C_2}+V_{C_4} = V_i \tag{5-56}$$

$$sC_2V_{C_2}-I_{L_1} = 0 \tag{5-57}$$

$$sL_3I_{L_3}+\frac{C_2}{C_3}V_{C_2}-\left[1+\frac{C_4}{C_3}\right]V_{C_4}-\frac{C_6}{C_3}V_{C_6} = 0 \tag{5-58}$$

$$sC_4V_{C_4}+I_{L_3}-I_{L_1}+I_{L_5}+sC_5(V_{C_4}-V_{C_6}-V_{C_7}) = 0 \tag{5-59}$$

$$sL_5I_{L_5}-V_{C_4}+V_{C_5}+V_{C_7} = 0 \tag{5-60}$$

$$sC_6V_{C_6}-sC_7V_{C_7}-I_{L_6}-\frac{V_{C_7}}{R_l} = 0 \tag{5-61}$$

$$sC_6V_{C_6}-I_{L_5}-sC_5(V_{C_4}-V_{C_6}-V_{C_7}) = 0 \tag{5-62}$$

$$sL_6I_{L_6}-V_{C_7} = 0 \tag{5-63}$$

Note that the third equation was obtained using the information from the cutset of V_{C_2}, V_{C_3}, V_{C_4} and V_{C_6} as shown above.

After substituting in the values of the capacitors, inductors and resistors in the above equations and putting all the derivatives of the states on the left side, the equations become: (In this example, five of the eight equations are already in the correct form)

$$sI_{L_1} = -0.1816I_{L_1} - 0.1816V_{C_2} - 0.1816V_{C_4} + 0.1816V_1 \tag{5-64}$$

$$sV_{C_2} = 3.855I_{L_1} \tag{5-65}$$

$$sI_{L_3} = -0.0414V_{C_2} + 2.2895V_{C_4} + 0.0534V_{C_6} \tag{5-66}$$

$$sI_{L_5} = 0.4914V_{C_4} - 0.4914V_{C_6} - 0.4914V_{C_7} \tag{5-67}$$

$$s(3.4955)V_{C_4} - s(0.3145)V_{C_6} - s(0.3145)V_{C_7} = I_{L_1} - I_{L_3} - I_{L_5} \tag{5-68}$$

$$-s(0.3145)V_{C_4} + s(0.6487)V_{C_6} + s(0.3145)V_{C_7} = I_{L_5} \tag{5-69}$$

$$s(0.3342)V_{C_6} - s(2.763)V_{C_7} = I_{L_6} + 0.5297V_{C_7} \tag{5-70}$$

$$sI_{L_6} = 2.0777V_{C_7} \tag{5-71}$$

Using the equations involving sV_{C_4}, sV_{C_6}, and sV_{C_7} to solve for sV_{C_4}, sV_{C_6}, and sV_{C_7} gives

$$sV_{C_4} = 0.2998I_{L_1} - 0.2998I_{L_3} - 0.1463I_{L_5} - 0.0089V_{C_7} - 0.0165I_{L_6} \tag{5-72}$$

$$sV_{C_6} = 0.1374I_{L_1} - 0.1374I_{L_3} + 1.3893I_{L_5} + 0.0838V_{C_7} + 0.1582I_{L_6} \tag{5-73}$$

$$sV_{C_7} = 0.0166I_{L_1} - 0.0166I_{L_3} + 0.1680I_{L_5} - 0.1816V_{C_7} - 0.3428I_{L_6} \tag{5-74}$$

The state space matrices are then written as

$$\mathbf{A} = \begin{vmatrix} -0.1816 & -0.1816 & 0 & -0.1816 & 0 & 0 & 0 & 0 \\ 3.855 & 0 & 0 & 0 & 0 & 0 & 0 & 0 \\ 0 & -0.0414 & 0 & 2.2895 & 0 & 0.0534 & 0 & 0 \\ 0.2998 & 0 & -0.2998 & 0 & -0.1463 & 0 & -0.0089 & -0.0165 \\ 0 & 0 & 0 & 0.4914 & 0 & -0.4914 & -0.4914 & 0 \\ 0.1374 & 0 & -0.1374 & 0 & 1.3893 & 0 & 0.0838 & 0.1582 \\ 0.0166 & 0 & -0.0166 & 0 & 0.1680 & 0 & -0.1816 & -0.3428 \\ 0 & 0 & 0 & 0 & 0 & 0 & 2.0777 & 0 \end{vmatrix} \quad \mathbf{b} = \begin{vmatrix} 0.1816 \\ 0 \\ 0 \\ 0 \\ 0 \\ 0 \\ 0 \\ 0 \end{vmatrix}$$

To find c, we note that V_{C_7} is the same as V_o so first

$$\mathbf{c}^T = [\,0\;0\;0\;0\;0\;0\;1\;0\,] \quad d = 0 \tag{5-75}$$

We can find the gain of the ladder transfer function at a reflection zero using fact that an LC ladder is designed to deliver maximum power transfer to the load at reflection zeros. The maximum power that can be delivered to the circuit on the load side of R_s is

$$P_{max} = \frac{|V_i|^2}{4R_s} \tag{5-76}$$

The power at the load is

$$P_{load} = \frac{|V_o|^2}{R_l} \tag{5-77}$$

Equating the two, and substituting in the values of R_s and R_l, we have the following

$$\frac{|V_i|^2}{4R_s} = \frac{|V_o|^2}{R_l} \tag{5-78}$$

so at the reflection zero

$$\frac{|V_o|}{|V_i|} = 0.6870 \tag{5-79}$$

Then, if we want to design our simulation so it has a gain of one at the reflection zeros, we multiply $\mathbf{c}$ by $\frac{1}{0.687}$ to get

$$\mathbf{c}^T = \begin{bmatrix} 0 & 0 & 0 & 0 & 0 & 0 & 1.4555 & 0 \end{bmatrix} \quad d = 0 \tag{5-80}$$

5.3 Scaling

The output signals of the integrators should be scaled to optimize the dynamic range of the filter. The output of an integrator can be adjusted by scaling all of its input resistors. Then so as to maintain the transfer function of the filter unchanged, any resistor that the adjusted integrator is connected to, must be inversely scaled. Equivalently, X_i in the state space system can be adjusted by multiplying the i'th row of $\mathbf{A}$ and $\mathbf{b}$ by a scaling factor and dividing

the i'th column of **A** and **c** by the same factor, as shown in chapter 2.

Two commonly used methods of scaling involve an L_∞ norm and an L_2 norm. The filter is then scaled for dynamic range by finding the appropriate norm of each integrator output, $f_i(s)$, or equivalently the norm of each capacitor voltage and inductor current simulated. The state space system is scaled by dividing the i'th row of **A** and **b** by state i's norm and multiplying the i'th row of $\mathbf{c}^T$ and the i'th column of **A** by the same norm. This scaling procedure results in $\|f_i\|_p = 1$ which means that we can apply as large a signal at the input (as measured by the p-norm) as the integrator outputs can accommodate.

The L_∞ norms of V_{C_1}, I_{L_2}, and V_{C_3} of the filter of figure 5.3 are 0.68, 0.87, and 0.5 respectively. The L_∞ scaled state space system of the above example is:

$$\mathbf{A} = \begin{bmatrix} -0.4828 & -0.4505 & -0.0961 \\ 1.1410 & 0 & -0.8390 \\ -0.1777 & 0.6127 & -0.4828 \end{bmatrix} \qquad \mathbf{b} = \begin{bmatrix} 0.7100 \\ 0 \\ 0.2613 \end{bmatrix} \tag{5-81}$$

$$\mathbf{c}^T = \begin{bmatrix} 0 \\ 0 \\ 1 \end{bmatrix} \qquad d = 0$$

This filter circuit is shown in figure 3.10 and was obtained using the equations in chapter 2.

The L_2 norms of the same functions above are 1.01, 1.518, and 0.708 respectively. The L_2 scaled state space system of this example is

$$\mathbf{A} = \begin{bmatrix} -0.4828 & -0.5292 & -0.0918 \\ 0.9713 & 0 & -0.6826 \\ -0.1859 & 0.7530 & -0.4828 \end{bmatrix} \qquad \mathbf{b} = \begin{bmatrix} 0.4791 \\ 0 \\ 0.1845 \end{bmatrix} \tag{5-82}$$

$$\mathbf{c}^T = \begin{bmatrix} 0 \\ 0 \\ 1.4163 \end{bmatrix} \qquad d = 0$$

5.4 Conclusions

Once the states have been chosen according to the guidelines in chapter 4 then we can use the procedures introduced in this chapter to obtain a state-space system. From this system, a circuit can be easily realized by following the procedure outlined in chapter 2.

Note that for a canonic ladder, we produce the same realization as that which would be obtained through the use of the leap-frog (or SFG) method. This realization for canonic ladders have been used extensively to simulate LC ladders and is known to have very good sensitivity properties.

The state-space simulation of non-canonic ladders use the original ladder as their basis and require no reciprocators as in the case of a SFG simulation. Also, no restriction is placed on the LC ladder prototype though if it is not a doubly-terminated LC ladder, then the rule-of-thumb of chapter 4 may not apply.

Introduced in this chapter were two methods to obtain the state-space matrices of a system which simulates an LC ladder. The matrix method is well-suited to CAD filter design as it can be easily programmed. An algebraic method was also provided for the case where a designer requires few filters and does not have the use of a computer.

6. CONCLUSIONS AND FUTURE RESEARCH

6.1 Conclusions

We have shown that, through the use of state-space filter synthesis, canonic realizations of LC ladders which maintain the low sensitivity properties of the ladder are possible. The state-space filter emulates N element voltage or current functions of the LC ladder, where N is the order of the desired transfer function. If the ladder prototype is canonic, then the resulting filter is the same as that obtained with the Leap-Frog or the SFG approach. If the ladder is non-canonic, then the choice of the N states is important as the filter can become unrealizable or have poor sensitivity and dynamic range properties. Some insight and a simple rule-of-thumb were presented to assist one in making this choice. The design methods of chapter four and five result in filters which compare favorably with other filter designs which simulate ladders.

Perhaps the most important feature of state-space filters is that their performance can be easily and accurately predicted. We saw in chapter 3 that the sensitivity predictions agreed quite closely with results obtained experimentally, including the effect of finite op-amp gain. As well, experimentally measured output noise voltage of a filter was shown to agree closely with theoretical prediction. These experimental results are the first to be reported for state-space filters.

6.2 Future Research

One area of considerable interest in industry today is the development of computer-aided design tools. There is presently a demand for software packages which assist an engineer in designing filters. There is an existing software package, Filtor2, which can be used to design a passive ladder prototype. It would then be quite useful to write a user-friendly program based on the method proposed in this thesis to obtain a scaled state-space system from the ladder, given the choice of states to be simulated. This program might go a step further and also produce a frequency scaled active RC circuit.

It would also be beneficial to apply the state-space design technique of this thesis to switched-capacitor (SC) filters. First though, one must find similar building blocks for positive and negative strays-insensitive SC integrators. Also, a practical requirement of present switched-capacitor filters is that the op-amp count be equal to or slightly larger than the order of the desired transfer function, N. It is not clear that one would be able to keep the op-amp count that low in a state-space filter. The author believes that a technique similar to capacitor-splitting might solve the op-amp count problem. Specifically, the method would be to use the initial equations written to describe the ladder to obtain a circuit realization. In the eighth order ladder example of chapter 5, these equations are (5-57)-(5-63). This approach would result in feed-in capacitors to integrators resulting in less feedback and feed-forward circuitry in the final circuit. A disadvantage of this approach is that many of the formulae of chapter 2 no longer apply since the filter would not be in state-space form.

High-frequency filters may be implemented in integrated circuits by using simple integrators with little or no feedback. The integrators would have very good frequency responses but would not be as precise as integrators with a lot of feedback, op-amp integrators. Since state-space filters are relatively insensitive to integrator-gains, they are ideally suited to this type of application.

Another interesting area to pursue is that of designing active high-pass filters. It seems backwards to design high-pass filters using blocks which are low-pass in nature, namely integrators. Perhaps a more sensible approach is to realize active high-pass filters with differentiators. One can apply most of the theory in chapter 2 to state-space filters which use differentiators as building blocks. As well, the method in chapter 5 need only be slightly modified to work with a system which contains differentiators rather than integrators.

1. REFERENCES

[1] W.M. Snelgrove, *Intermediate- function Synthesis*, Ph.D. Thesis, University of Toronto, Toronto, Canada 1982

[2] H.J. Orchard, "Inductorless Filters", *Electron Lett.*, vol. 2, pp.224-225, June 1966

[3] F.E.J. Girling and E.F. Good, "Active filters 12: The Leap-Frog or active ladder synthesis", *Wireless World*, Vol. 76, pp. 341-345, July 1970.

[4] P.O. Brackett and A.S. Sedra, "Direct SFG Simulation of LC Ladder Networks with Applications to Active Filter Design", *IEEE Trans. Circuits and Systems*, vol. CAS-23, pp. 61-67, Feb. 1976.

[5] K. Martin, *High- Order Bandpass Active Filters*, M.A.Sc. Thesis, University of Toronto, Toronto, Canada, 1977.

[6] L.T. Bruton, "Filter synthesis using generalized impedance converters", *Proc. NATO Advanced Institute of Signal and Network Theory*, Bournemouth, England, Peter Peregrinus, London 1973.

[7] G.M. Jacobs, D.J. Allstot, R.W. Brodersen, and P.R. Gray, "Design techniques for MOS switched capacitor ladder filters", *IEEE Trans. Circuits Syst.*, vol. CAS-25, pp. 1014-1021, Dec. 1978.

[8] G. Szentirmai, "Synthesis of Multiple-Feedback Active Filters", *Bell Syst. Tech. J.*, vol. 52, pp. 527-555, Apr. 1973.

[9] C.T. Mullis and R.A. Roberts, "Synthesis of Minimum Roundoff Noise Fixed-point Digital Filters", *IEEE Trans. Circuits and Systems*, vol. CAS-23, pp. 551-562, Sept. 1976.

[10] W.M. Snelgrove, *FILTOR2 User's Manual*, University of Toronto, 1980.

[11] P.O. Brackett and A.S. Sedra, "Active Compensation for High-Frequency Effects in op-amp circuits with Applications to Active-RC Filters", *IEEE Trans. Circuits and Systems*, CAS-23, pp.68-73, Feb. 1976.

[12] W. Kaplan, *Advanced Calculus*, Addison-Wesley, 1952.

[13] A.S. Sedra and P.O. Brackett, *Filter Theory and Design: Active and Passive*, Matrix Publishers, Champagne, Illinois, 1978.

[14] M.S. Ghausi and K.R. Laker, *Modern Filter Design*, Prentice Hall, Englewood Cliffs, NJ, 1981.